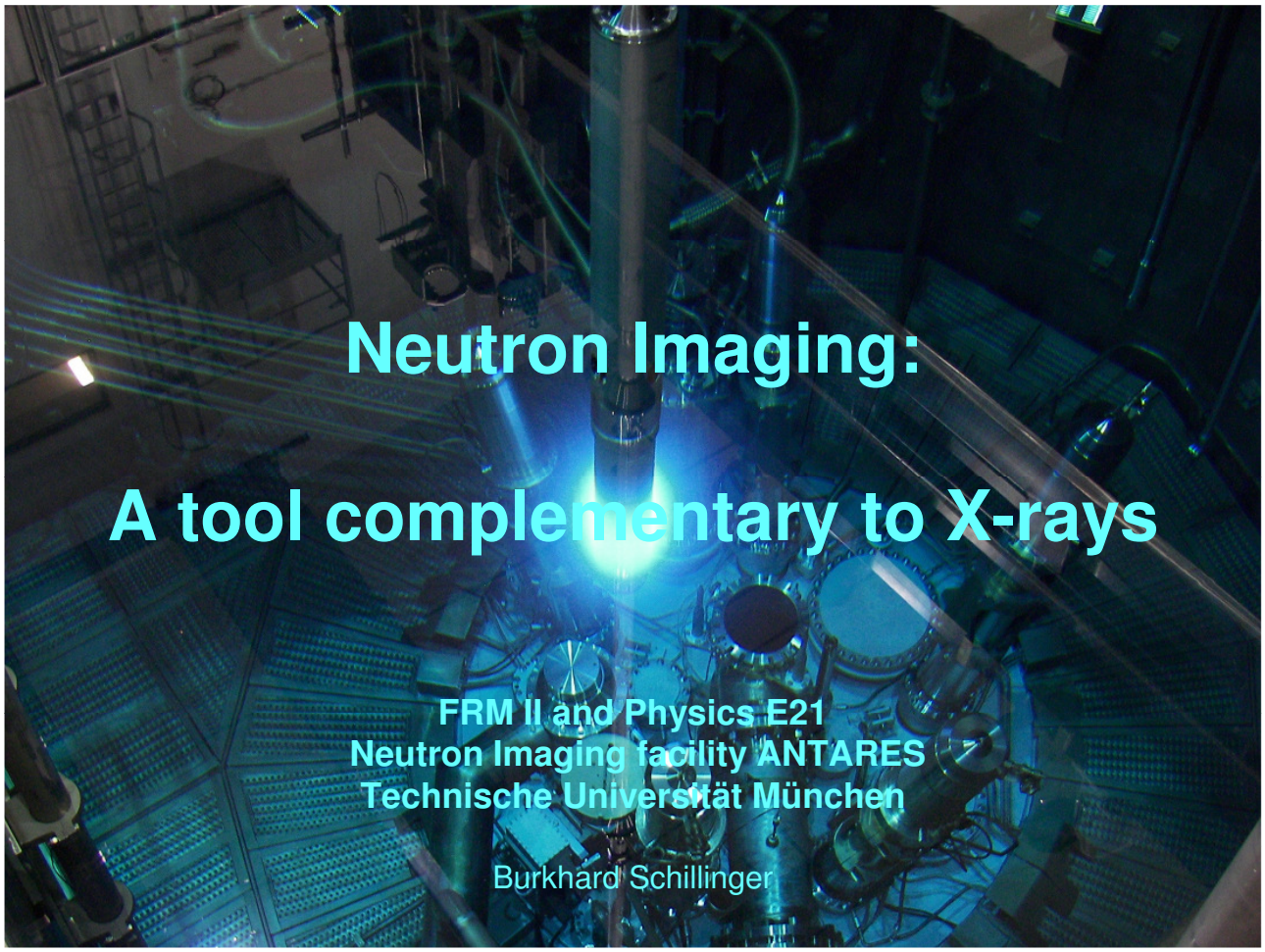

# Neutron Imaging:

# A tool complementary to X-rays

FRM II and Physics E21
Neutron Imaging facility ANTARES
Technische Universität München

Burkhard Schillinger



**Why use Neutrons?**

**Compare interaction of X-rays and Neutrons with matter**

**Where to get neutrons from: Fast and thermal/cold neutrons**

**Examinations with fast neutrons**

**Examinations with thermal/cold neutrons:**

- **Radiography**
- **Computed tomography**
- **Dynamic imaging**
- **Phase contrast imaging**
- **Monochromatic imaging**
- **Dark field scatter imaging**

## X- and gamma-rays

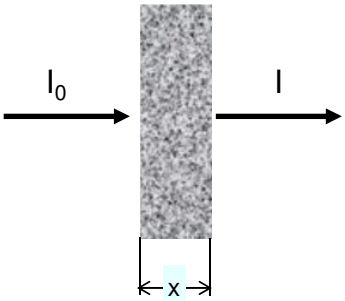


## X- and gamma-rays

Some “physics”: X-rays and gamma-rays interact with the electrons of the atoms basically via

- photoelectric effect,
- Compton effect and
- pair production





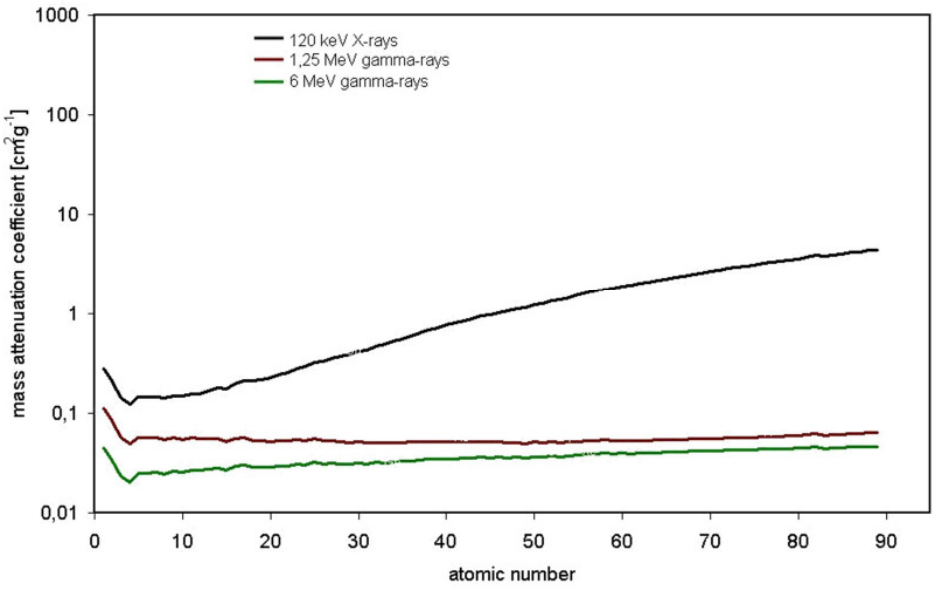


**The more electrons (i.e. the higher the atomic number) the higher the probability for interaction.**
**⇨ Increase of mass attenuation coefficient (μ/ρ) with increasing atomic number**

**The higher the energy of X-rays and gamma-rays the less the probability for interaction.**
**⇨ Decrease of mass attenuation coefficient (μ/ρ) with increasing energy**

## Neutrons

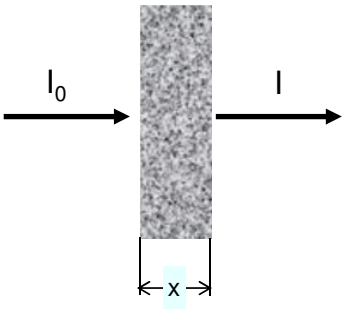


Some "physics": Neutrons interact with the nuclei of the atoms basically via

- nuclear reactions,
- elastic scattering and
- inelastic scattering

Scattering may occur as
- incoherent scattering on single nuclei,

and, for thermal and cold energies,

- coherent scattering on lattices.





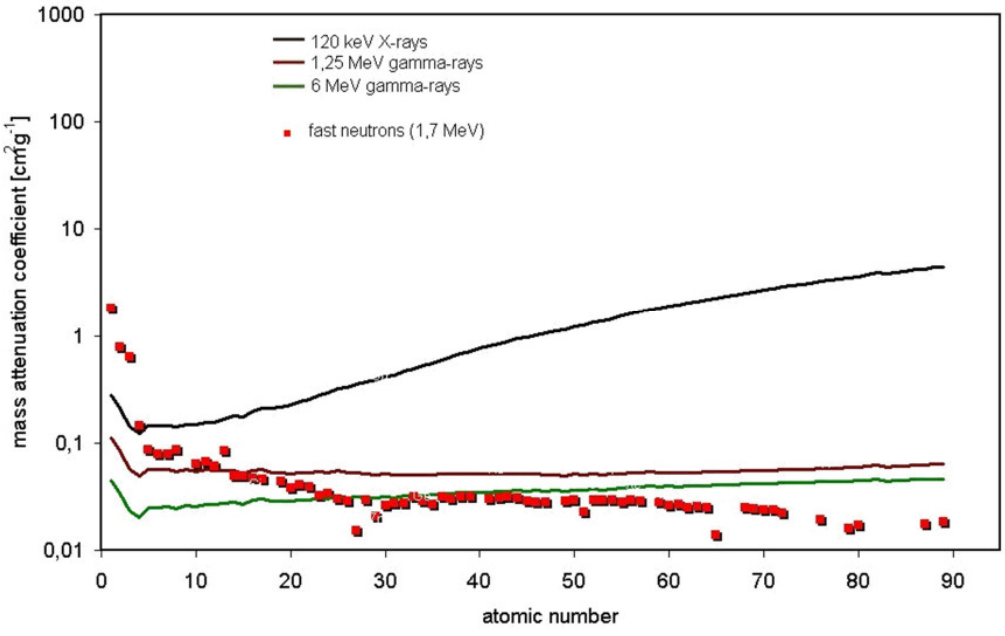


Fast neutrons interact basically via scattering
⇒ Decrease of mass attenuation coefficient (μ/ρ) with increasing atomic number

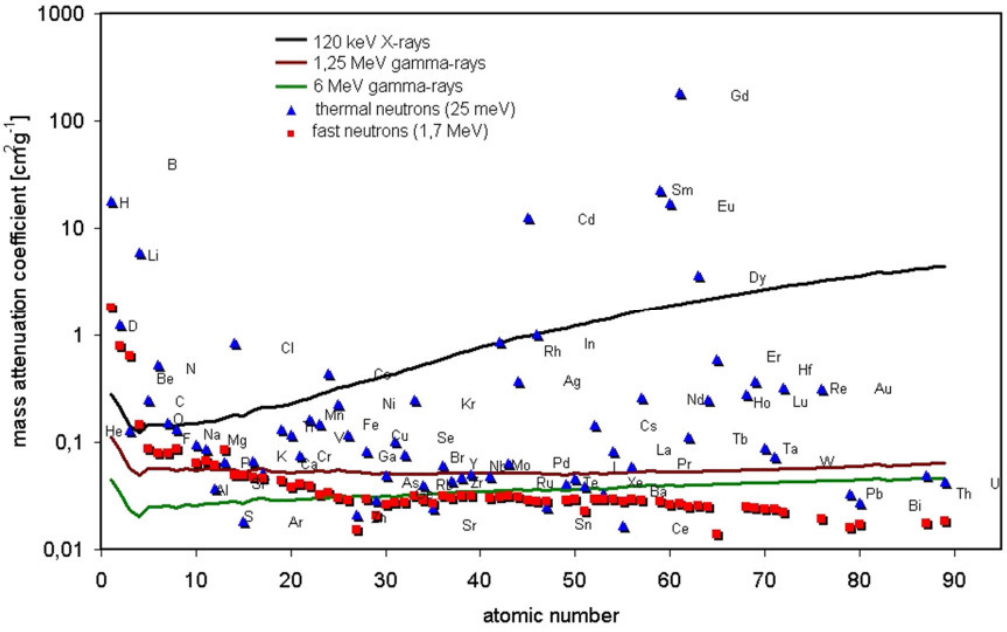


Thermal neutrons interact basically via nuclear reactions (capture) and scattering.
 Probability for interaction depends on the internal structure of the nucleus.
Therefore no simple regularity exists.





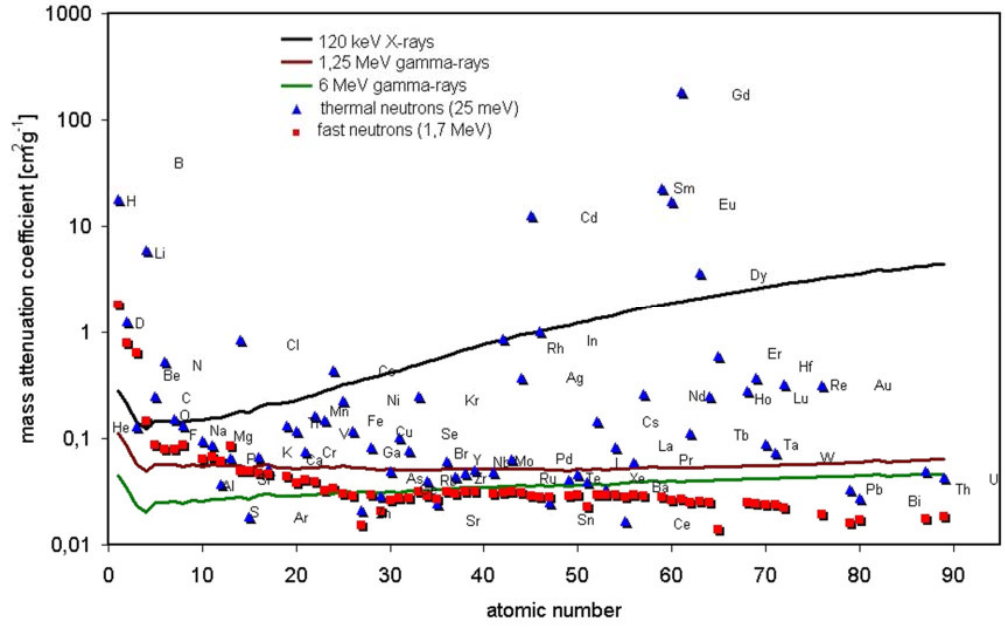


- High penetration for fast neutrons on heavy materials
- High contrast for hydrogen for fast and thermal neutrons  organic matter
- Good penetration for Al, Fe, Cu, Pb  technical metal samples
- Good contrast for many light elements
- Extremely high contrast for Gd  Use of contrast agents

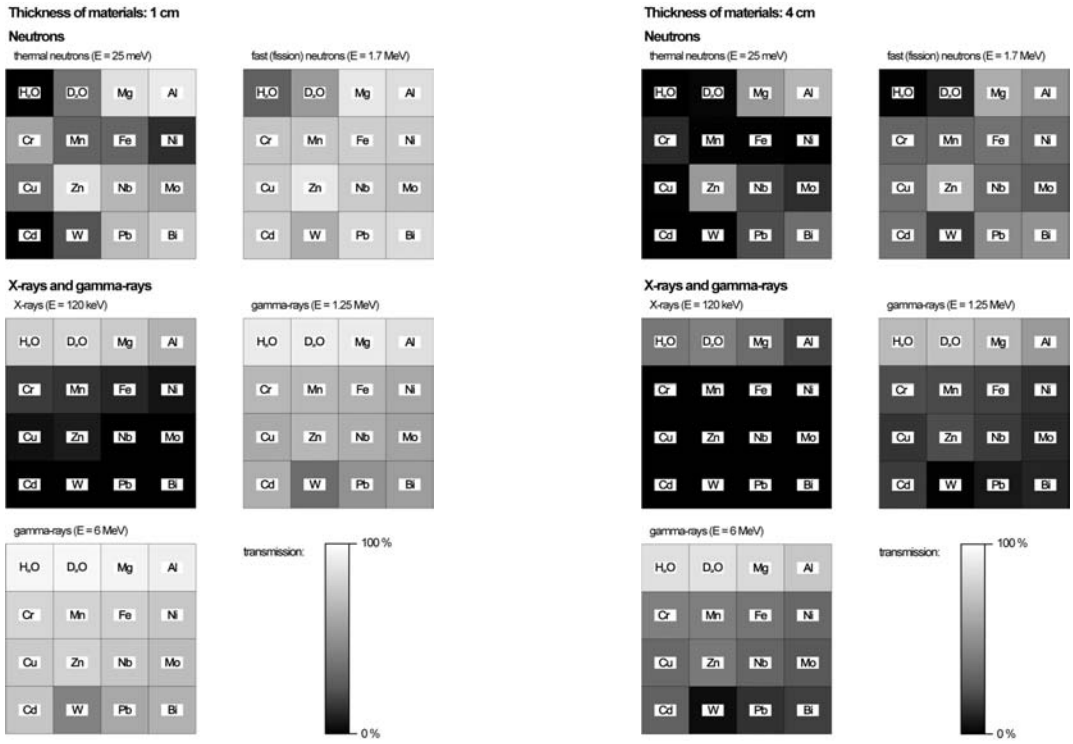






# Neutrons

→ nucleons

→ neutral

→ 10.000 times smaller than atoms

→ penetrate massive matter

→ rich in contrast

→ Wavelength λ = 0,05 ... 100 nm

→ magnetic moment (compass needle)

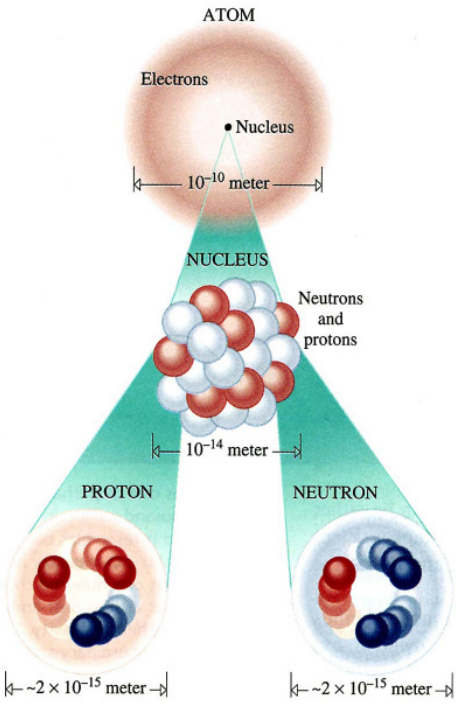

# How to get free neutrons?



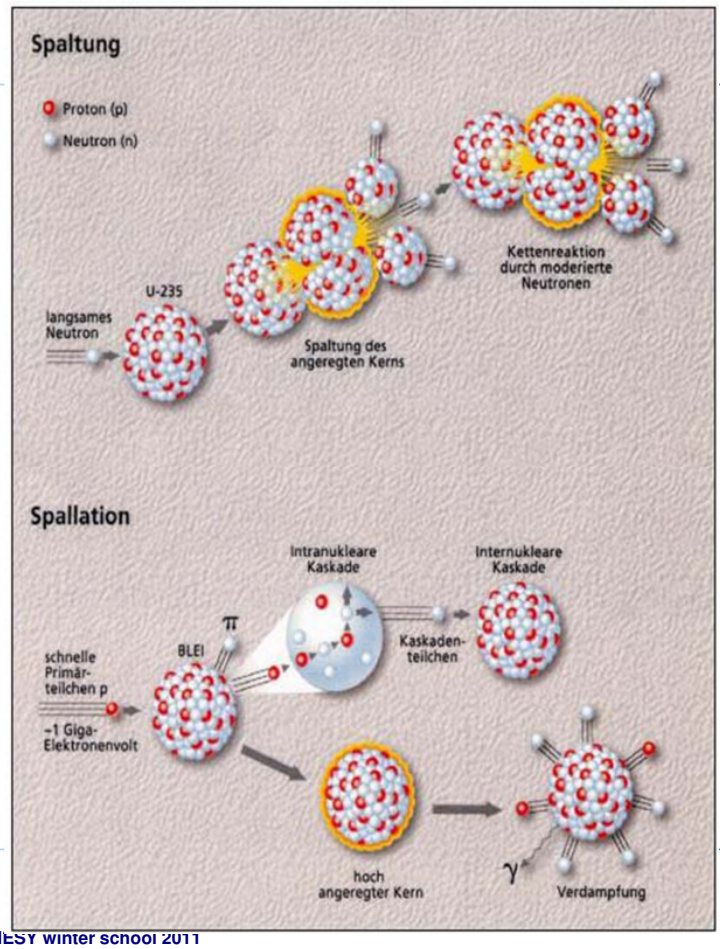




## Fission

$^{235}U + n_{therm.} \rightarrow$

Fission products + $2{,}4n_{fast}$ + 200 MeV

Spallation

$p^{+}$ (GeV) + Heavy target $\rightarrow$

Evaportion of ca. $10n_{fast}$

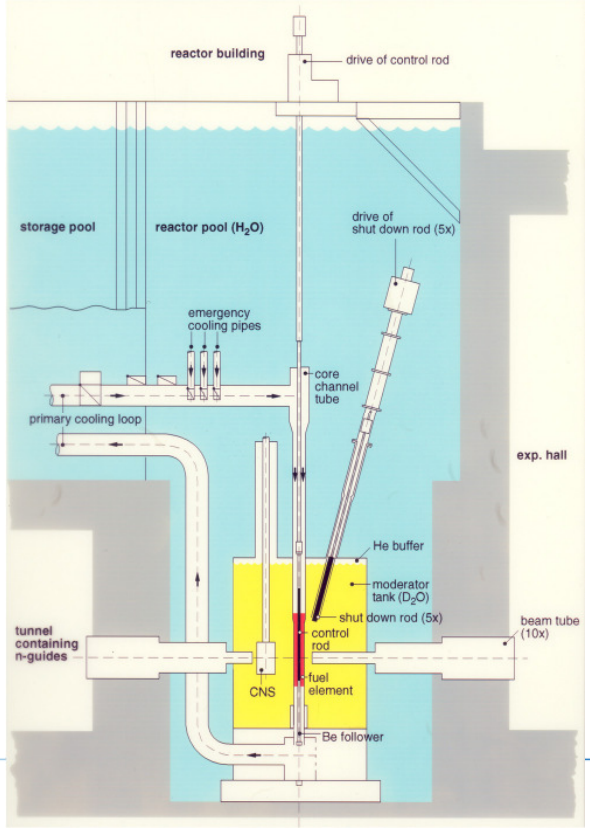


# Schematic construction of the neutron source

- Compact fuel element with Uranium silicide
  ( ~ 8kg Uranium, 93% enrichment)
- Heavy water moderator
- Thermal power 20 MW
- Primary cooling cycle with light water
- Two independent shutoff systems
- Biological shielding by 1.25m water and 1.5m heavy concrete sideways, and 10m water upwards





# Cross section of the reactor block

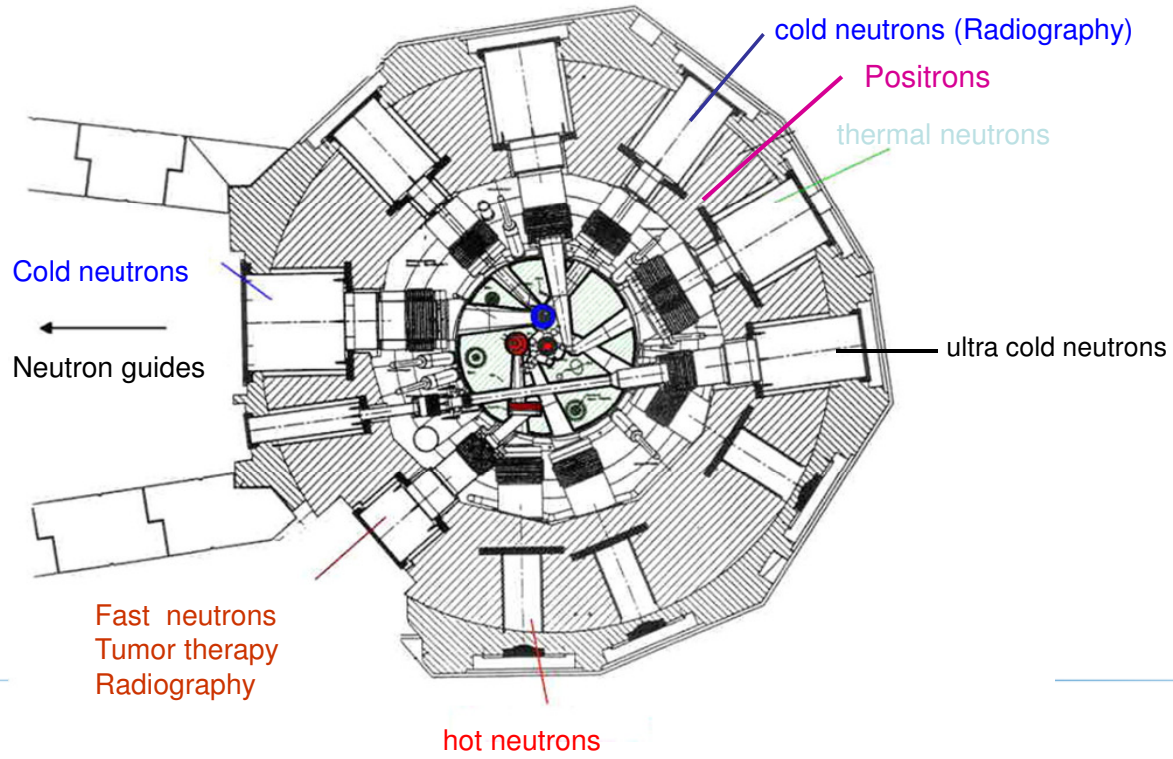

# Secondary neutron sources

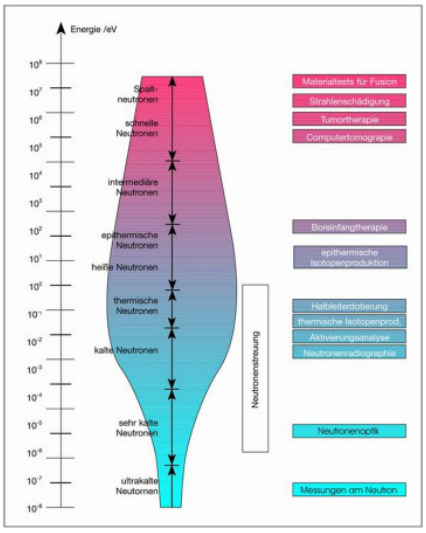


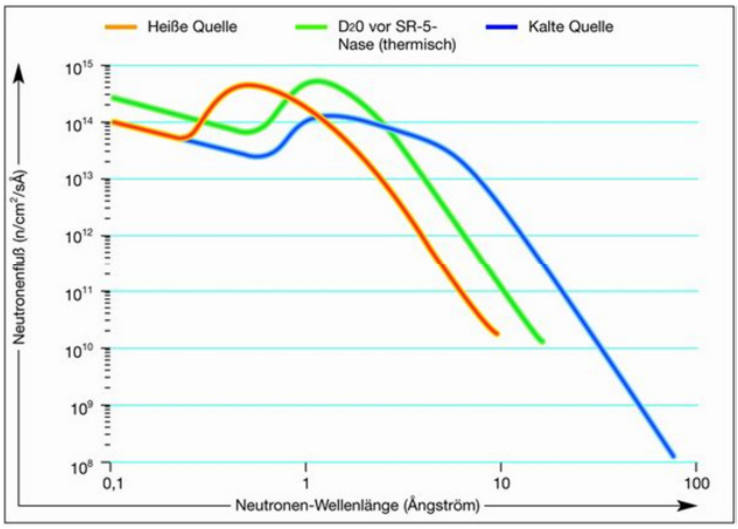


By secondary sources, the energy spectrum of the available neutrons is shifted and optimized for the according applications.





# Converter facility for the generation of high-energy fission neutrons

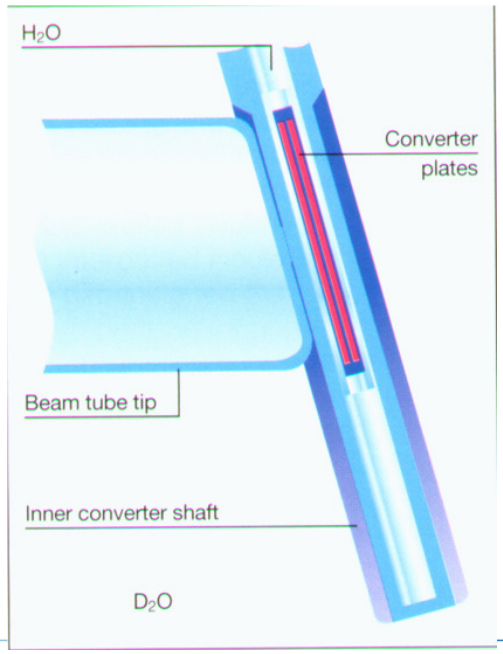


Technical data:

- Outer dimensions
  176 · 250 · 3.26 mm³
- 270g U (as $U_3Si_2$) 93% enriched
- Thermal total power ~ 80kW
- Cooling water throughput 33m²/h
- Flux of fast neutrons
  $1.5 \cdot 10^9$ n/cm²/s

## Radiography and Tomography with Fission Neutrons: The NECTAR facility

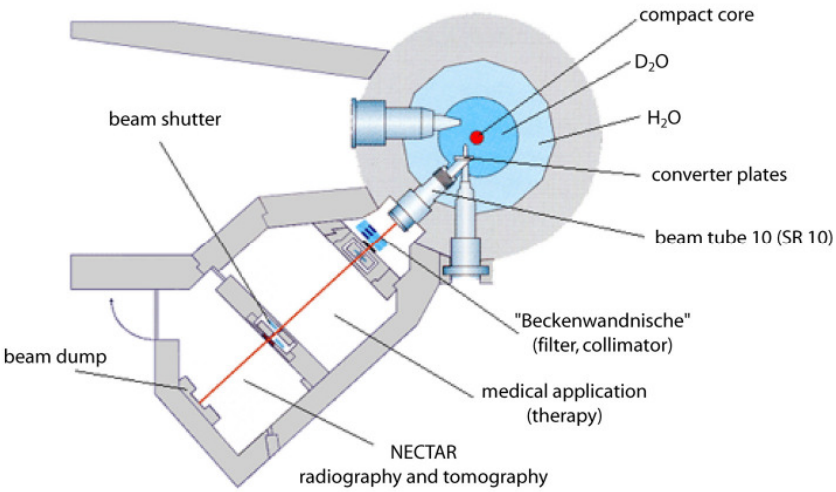






## Radiography and Tomography with Fission Neutrons

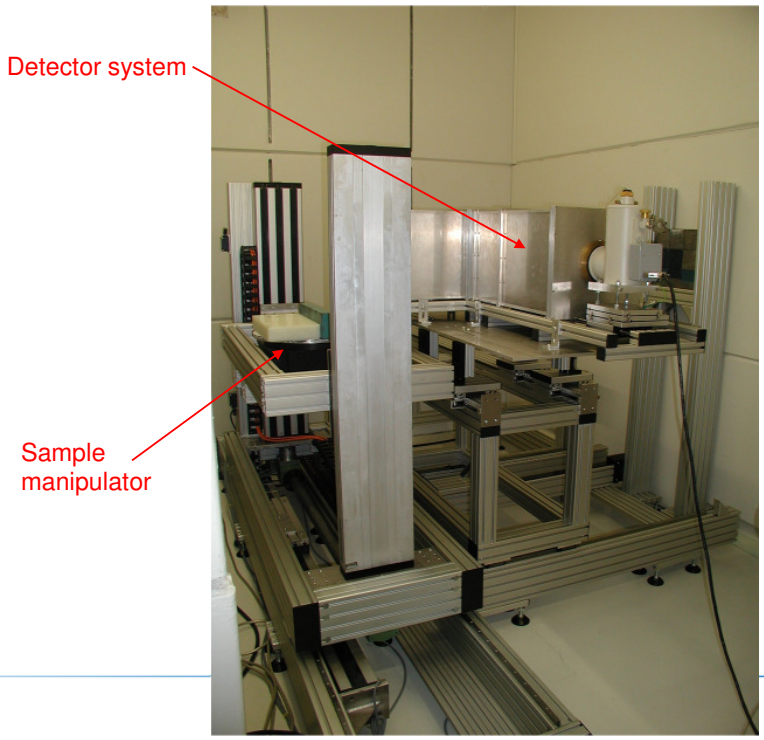


**NECTAR**
(**NE**utron **C**omputerized **T**omography **A**nd **R**adiography)

Technical Data:

Maximum sample dimensions:
80 cm x 80 cm x 80 cm
400 kg

Neutron beam:
max. $6.4 \cdot 10^7$ $cm^{-2} \cdot s^{-1}$

Typical measuring time for
Radiography: a few minutes
Tomography: several hours

Resolution: 0.5 mm - 1 mm

# Investigation of technical samples

## Oil distribution within a gear box





# Investigation of technical samples

## Oil distribution within a gear box

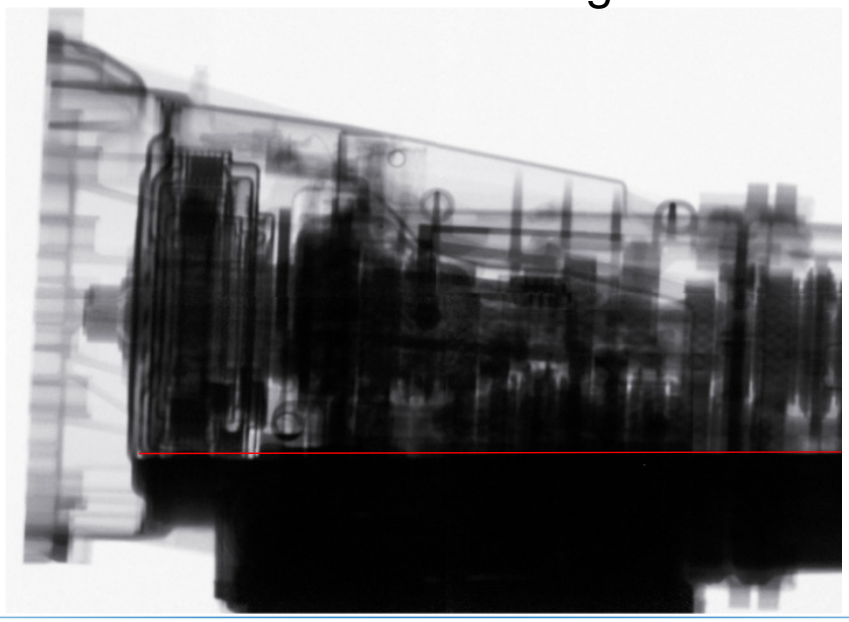

# Investigation of technical samples

## Hydraulic motor of an excavator

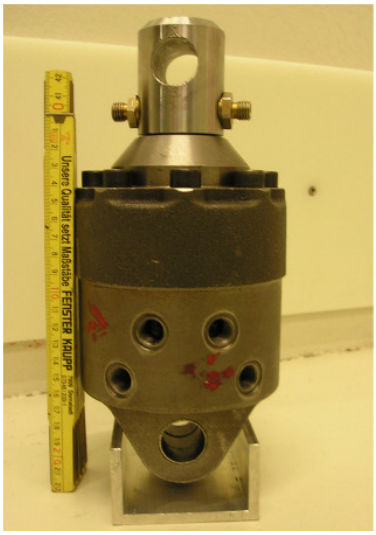






# Investigation of technical samples

## Hydraulic motor of an excavator

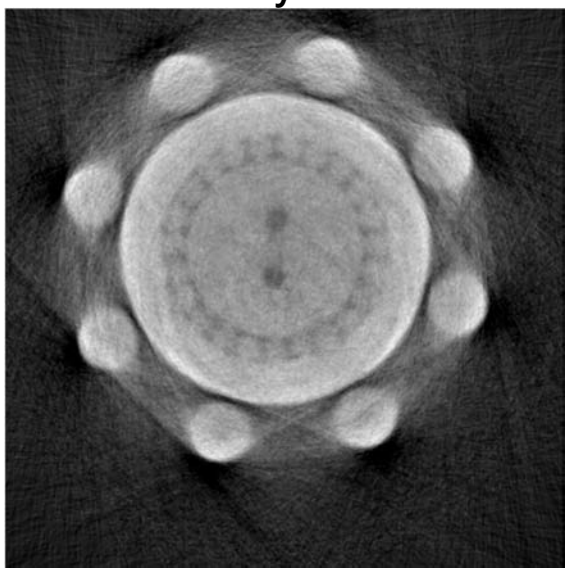

2D-CT

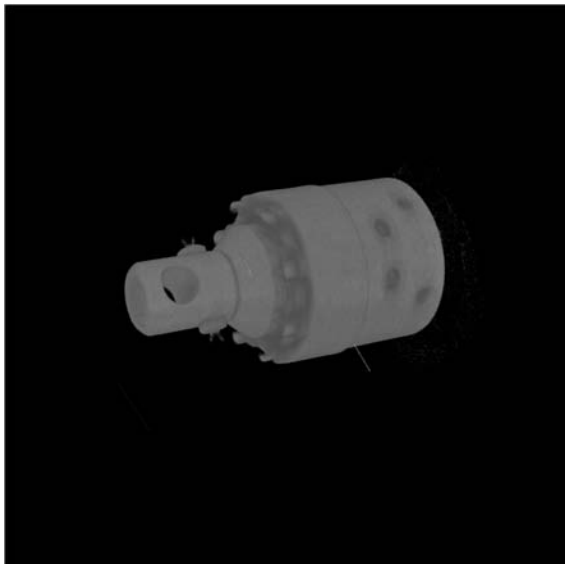

3D-CT

# Tomography with thermal neutrons

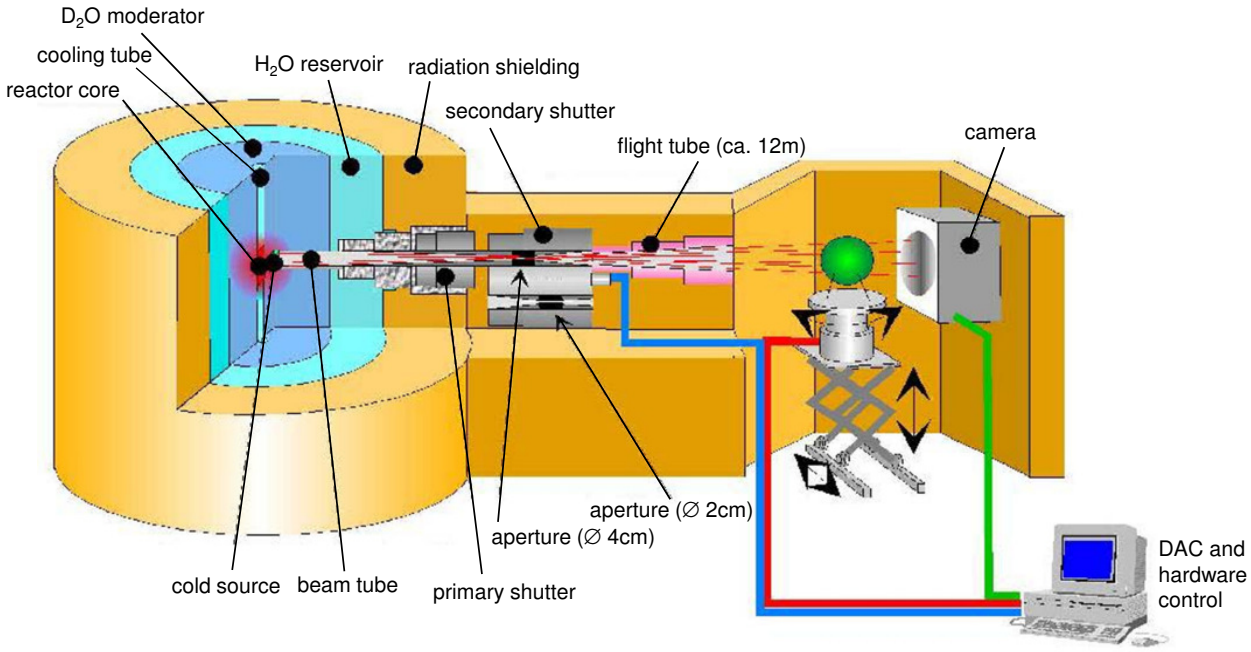






# *Antares*

**A**dvanced **N**eutron **T**omography **A**nd **R**adiography **E**xperimental **S**ystem

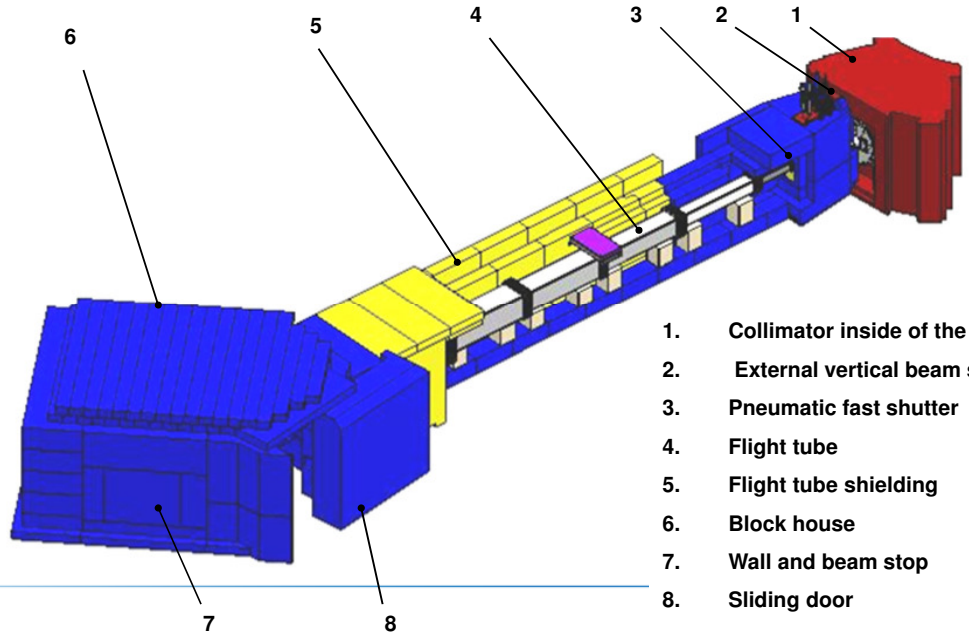


1. **Collimator inside of the biological shielding**
2. **External vertical beam shutter**
3. **Pneumatic fast shutter**
4. **Flight tube**
5. **Flight tube shielding**
6. **Block house**
7. **Wall and beam stop**
8. **Sliding door**




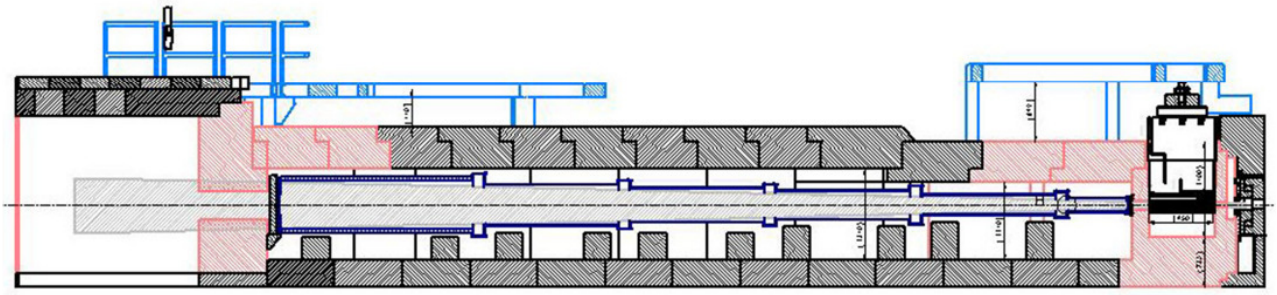

Cross section of the ANTARES facility.





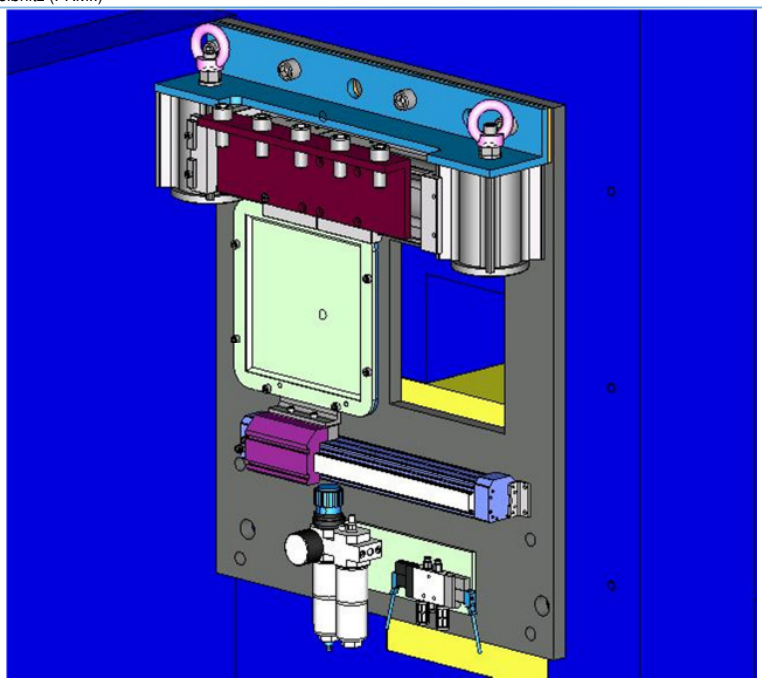

A pneumatic fast shutter at the beginning of the flight tube is used to shut off the thermal beam between exposures in order to minimize activation of the sample .

# Limitations in image resolution

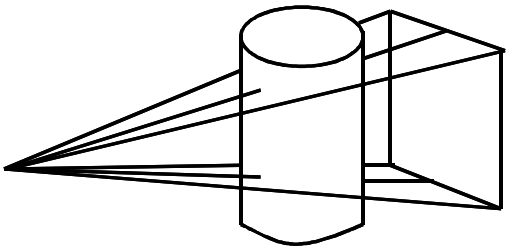

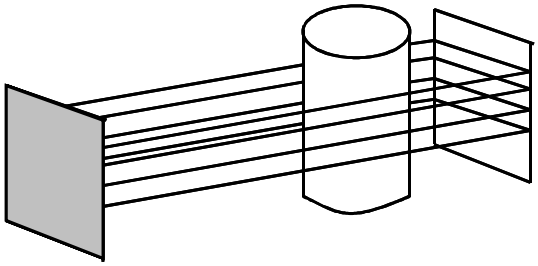

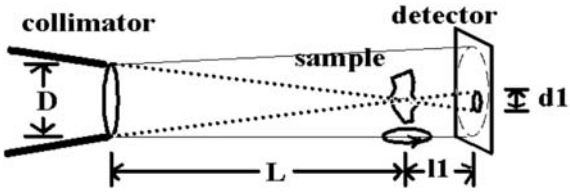


X-rays:Cone beam geometry
Inherent magnification by projection
High resolution image with
medium resolution detector

Neutrons: quasi-parallel beam geometry
No inherent magnification
Detector resolution equals
image resolution





# The limit is in the ZnS+$^{6}$LiF scintillation screen!

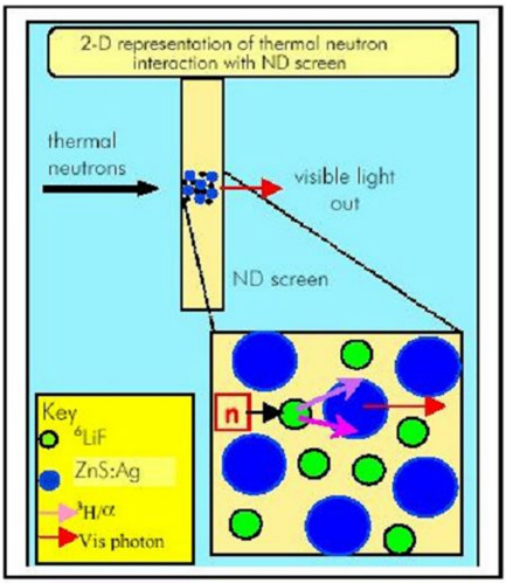


The reaction products of

$^{6}Li(n,\alpha)^{3}H + 4.7$ MeV

have to be stopped in the ZnS scintillation screen.
Their average range is in the order of 50-80 µm.

With thinned scintillation screens, we can achieve in the order of 20-30 µm.

# Good metal penetration: Radiography of a Roman Statue

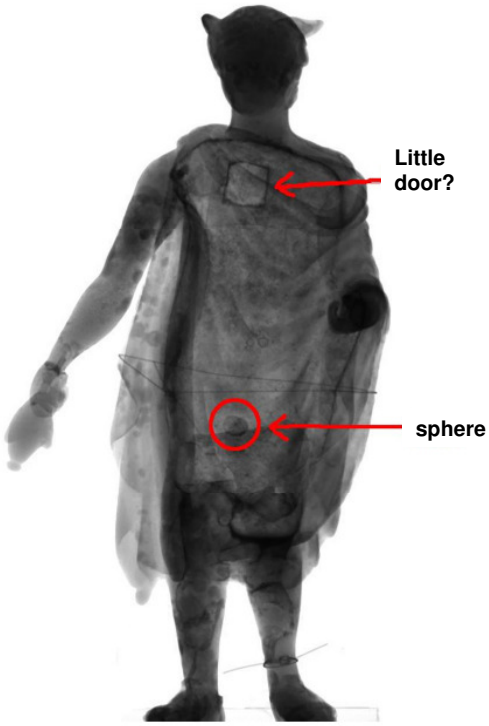






## Good metal penetration and high hydrogen contrast: A diesel injector pump

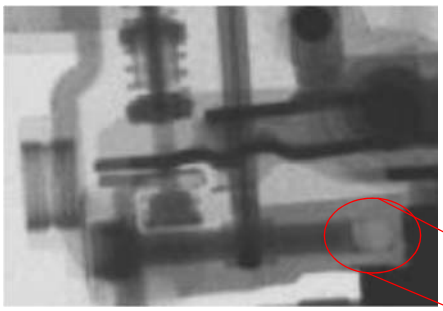

Oil remains

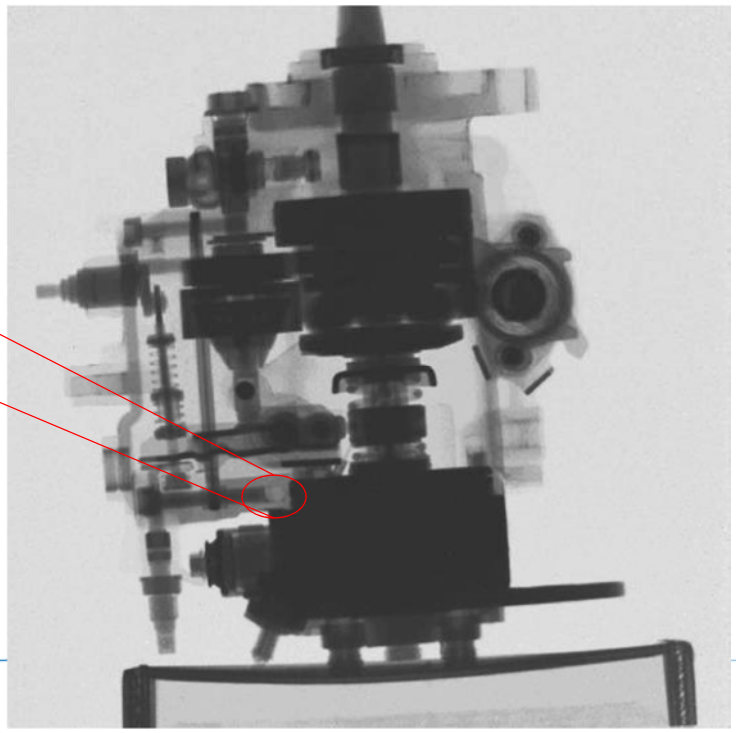

Good metal penetration and high hydrogen contrast:

A gas pressure reducer with sealants and o-rings

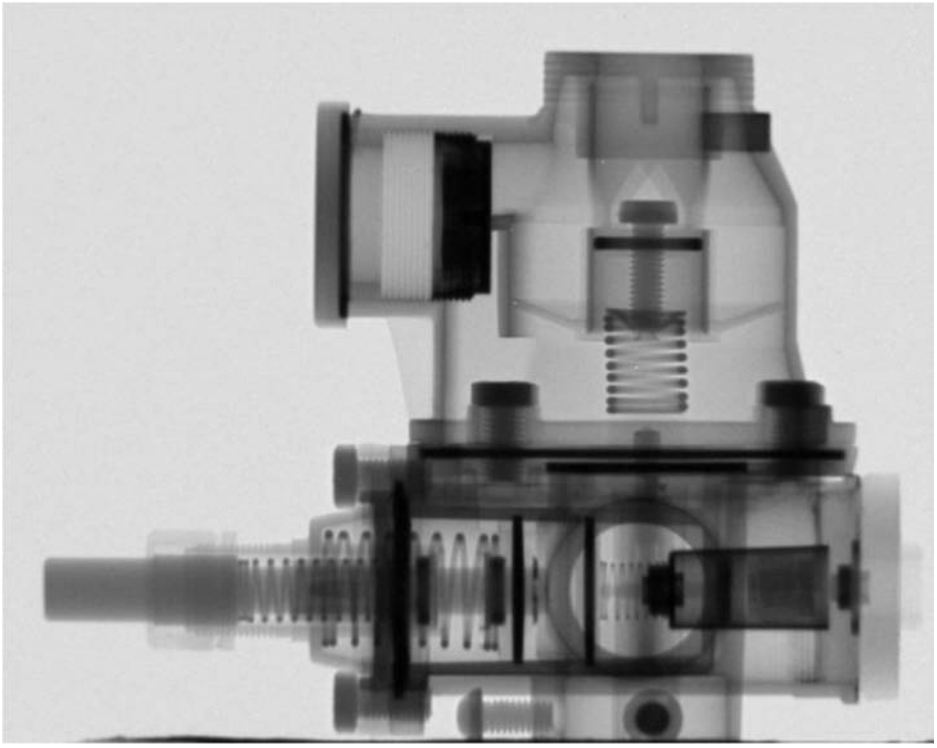



Good metal penetration and high hydrogen contrast:
A gas pressure reducer with sealants and o-rings

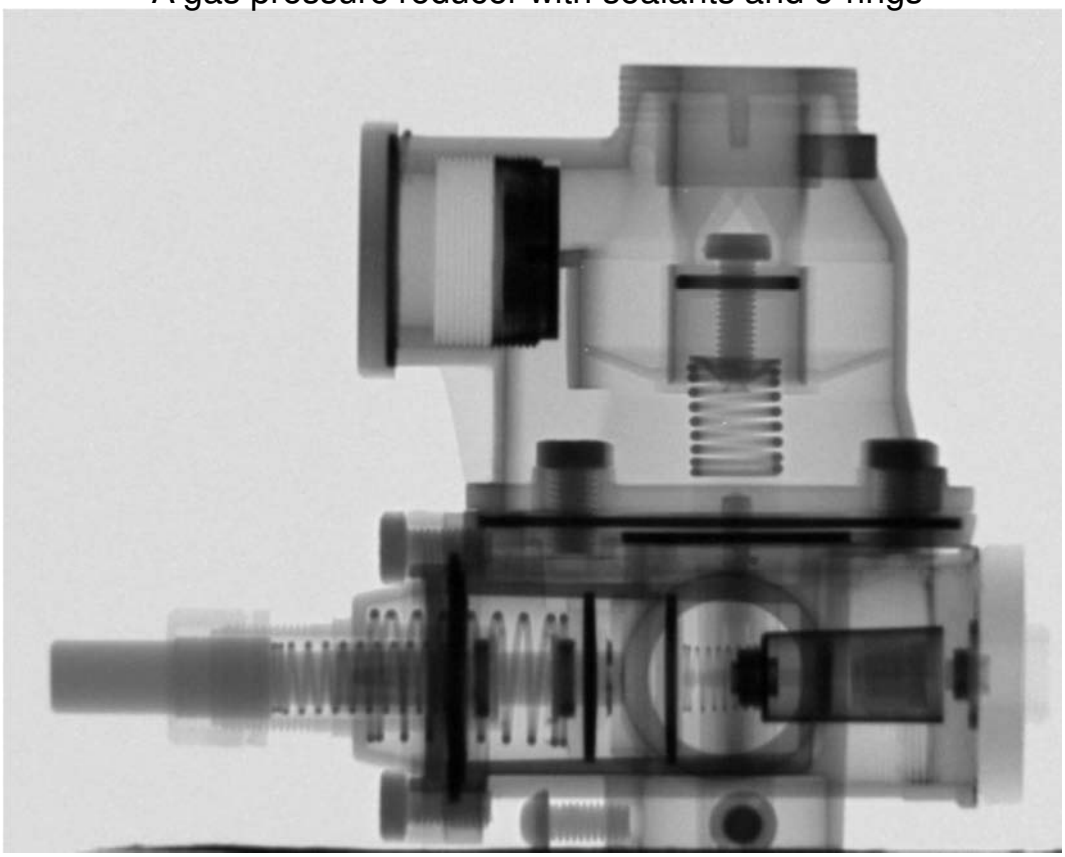

Good metal penetration and high hydrogen contrast: Glue sealants in a car door

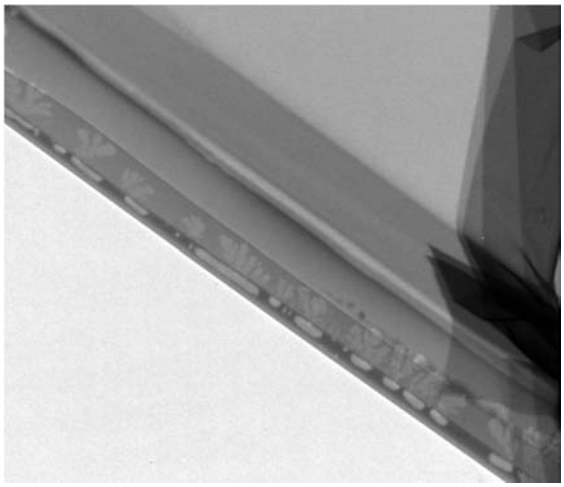





# Casting simulation:
# Evaporation of moisture in cast form sand

- Casting form sand (Bentonite) contains moisture in-between the grains as well as in layers within the Bentonite.

- The evaporation during casting deteriorates the Bentonite.

- The sand can be partially recycled, ading some fresh sand and water every time.

- Understanding the evaporation process helps to optimize the recycling.

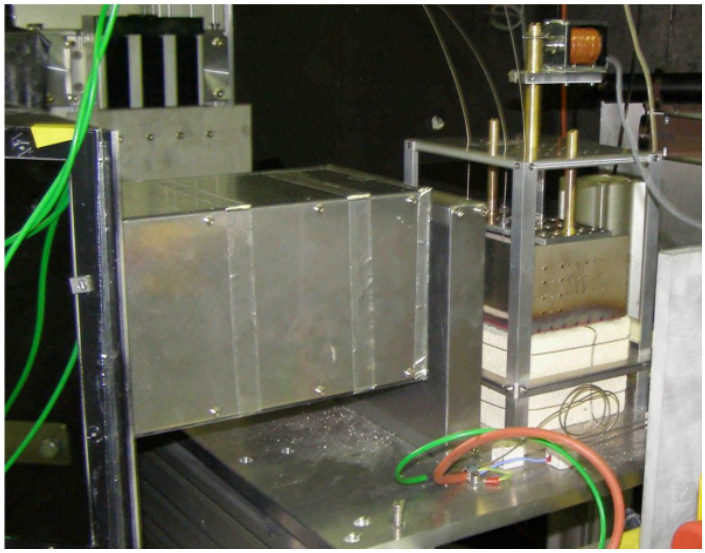

- A block of moist form sand is dropped on a red-hot copper plate
- Moisture evaporates in two fronts:
First the moisture between grains,
then the layered moisture within the grains

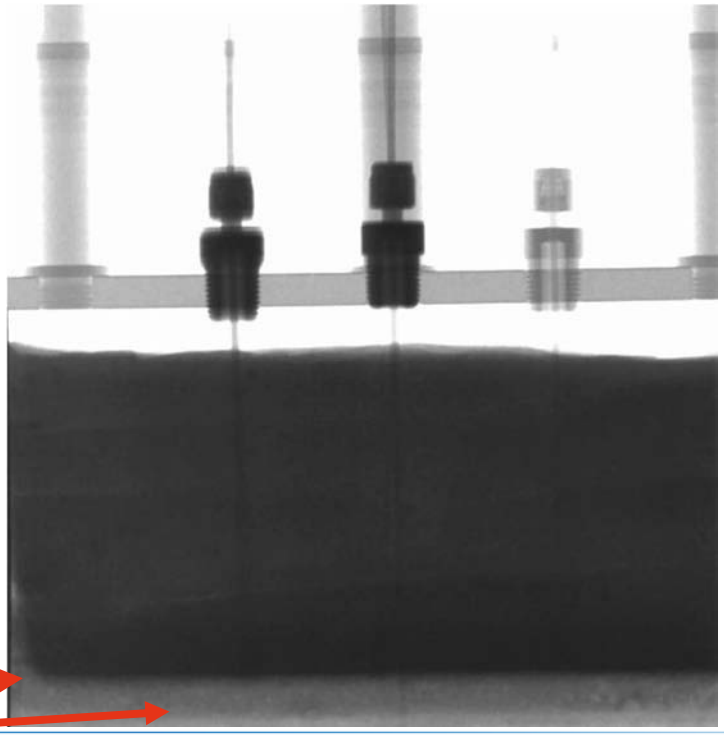






- A block of moist form sand is dropped on a red-hot copper plate
- Moisture evaporates in two fronts:
First the moisture between grains,
then the layered moisture within the grains

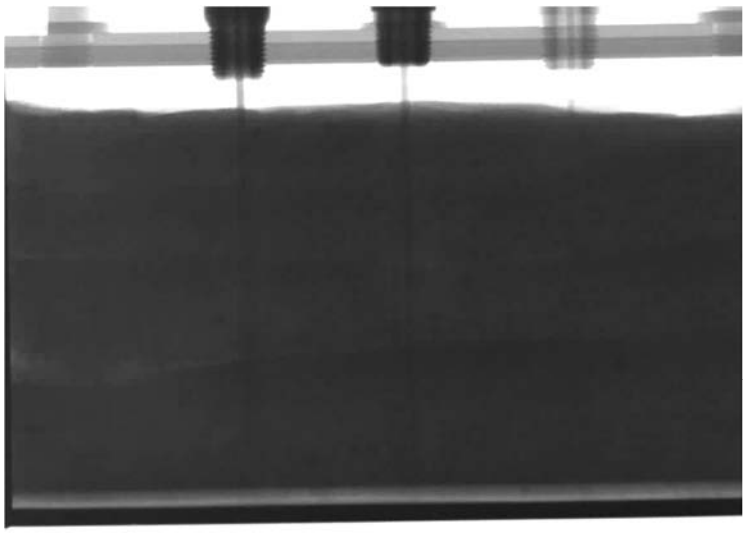

# Some technical examples

The German Federal Police built this tube bomb for us - without real explosives. The steel tube has 8 mm thickness.





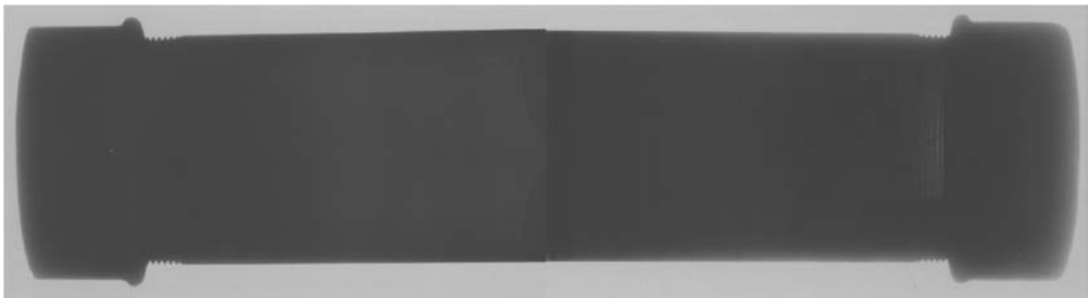

150 kV X-rays can hardly penetrate the wall.

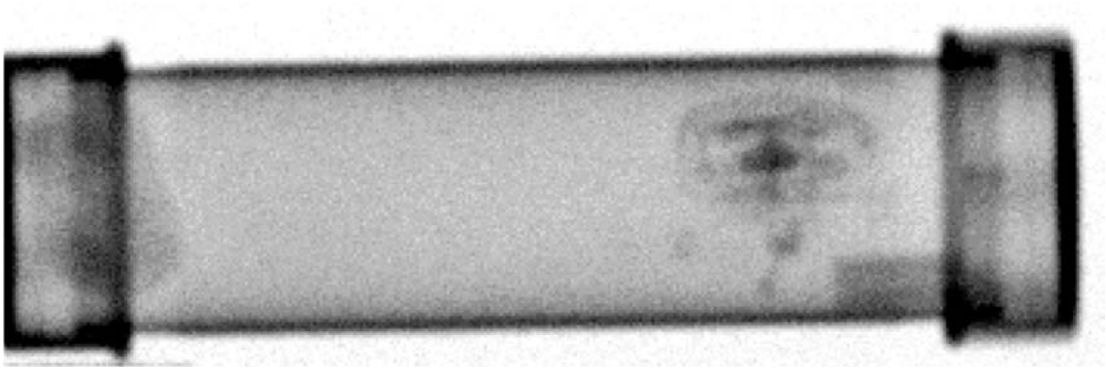

For hard gamma radiation (Cobalt-60, 1.2 MeV),
the steel tube becomes transparent, but also the contents.





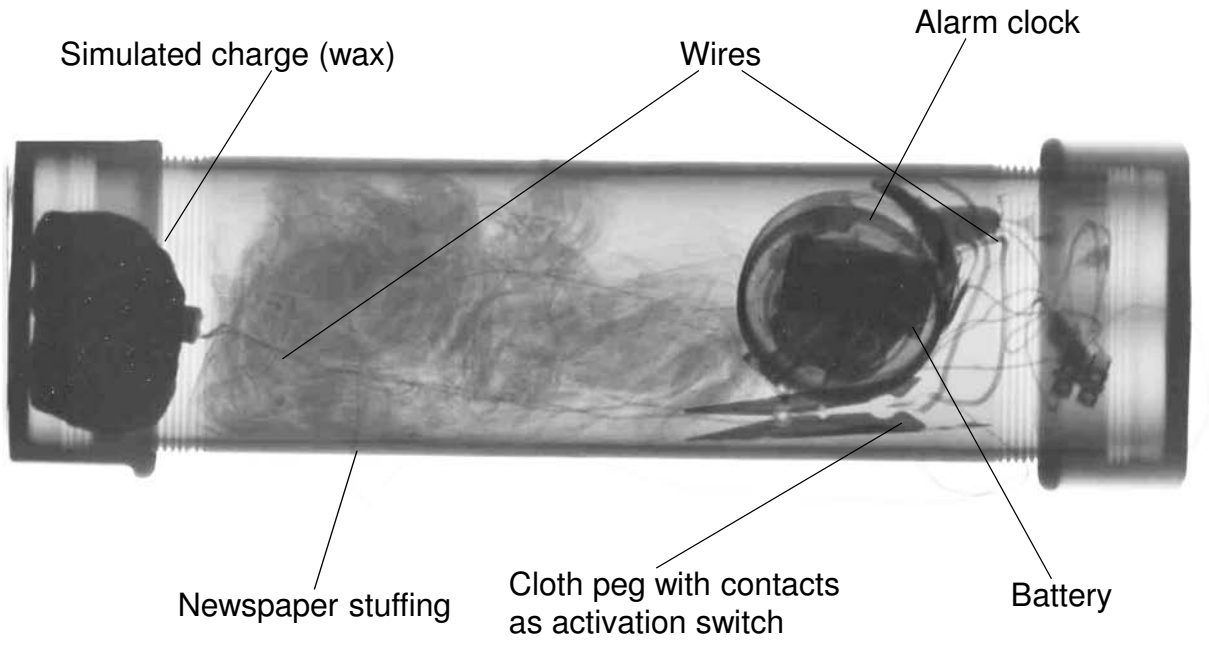


Thermal neutrons reveal much more!

# Sealed Roman vase/amphora, presumed empty.





# A neutron radiography and tomography reveals plant seeds!

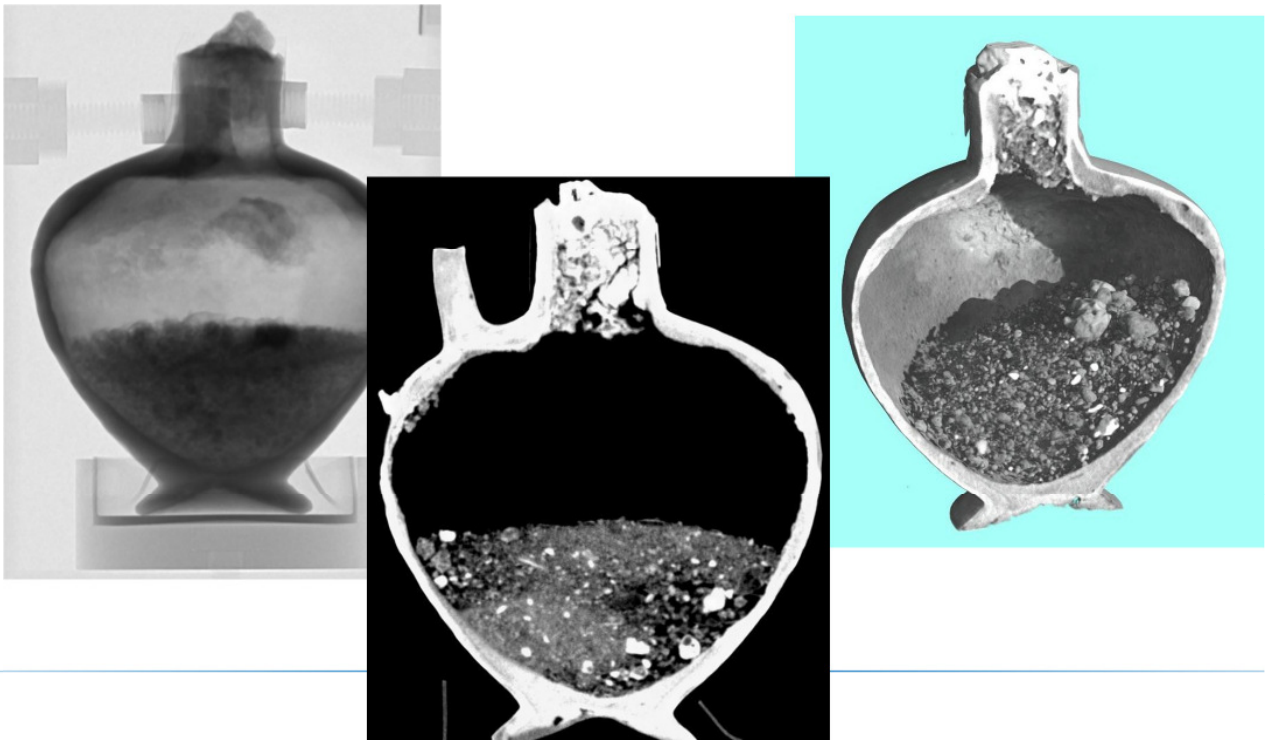

# Extension: X-ray tube for overlaying images

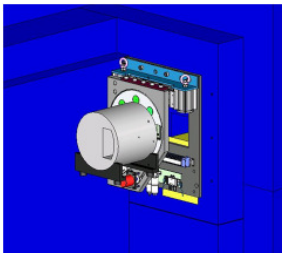

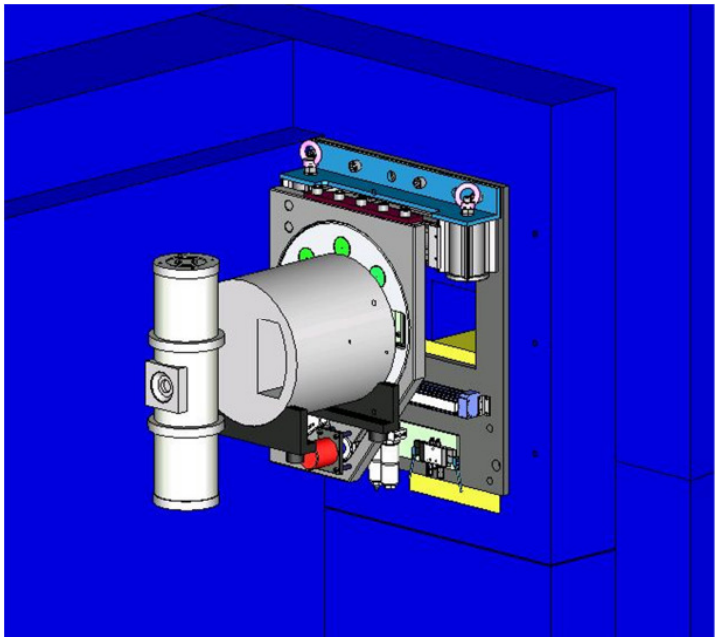

A removable 320 kV X-ray tube has been mounted before the flight tube.
This allows for alternate X-ray tomography in the identical beam geometry!





## Comparison and combination of X-ray and neutron images

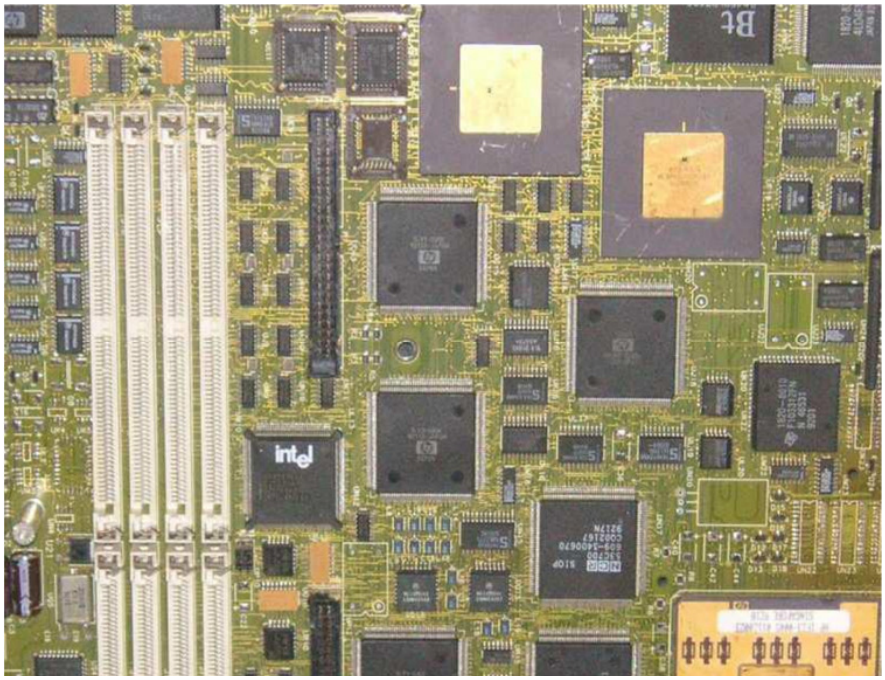


Images
M. Schulz,
TUM

Photo of a printed circuit board.
Note many parts with plastic or ceramic cases and lots of pins.

## Comparison and combination of X-ray and neutron images

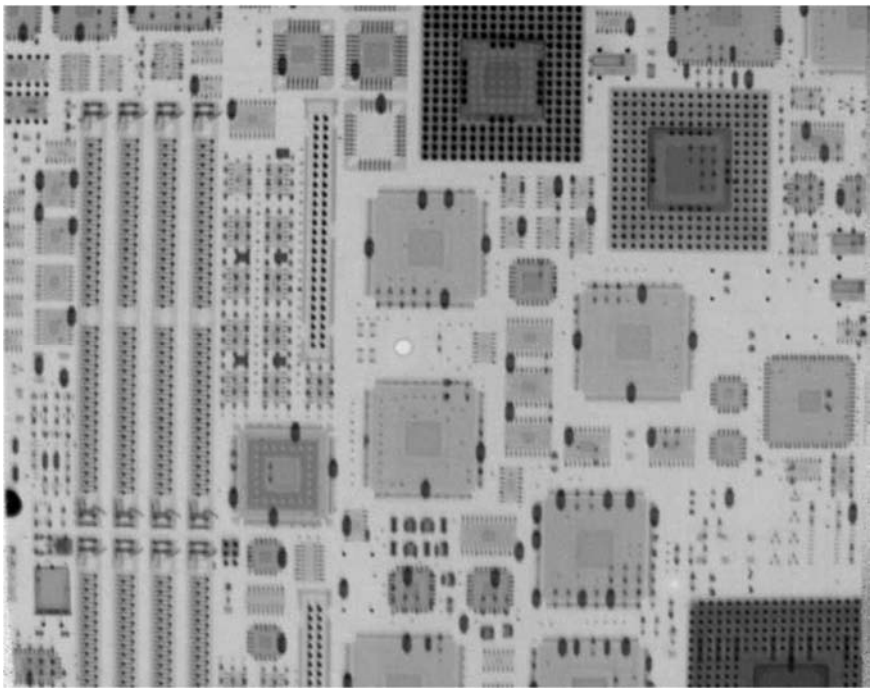

X-ray image.
Most contrast is given by the metal pins.





## Comparison and combination of X-ray and neutron images

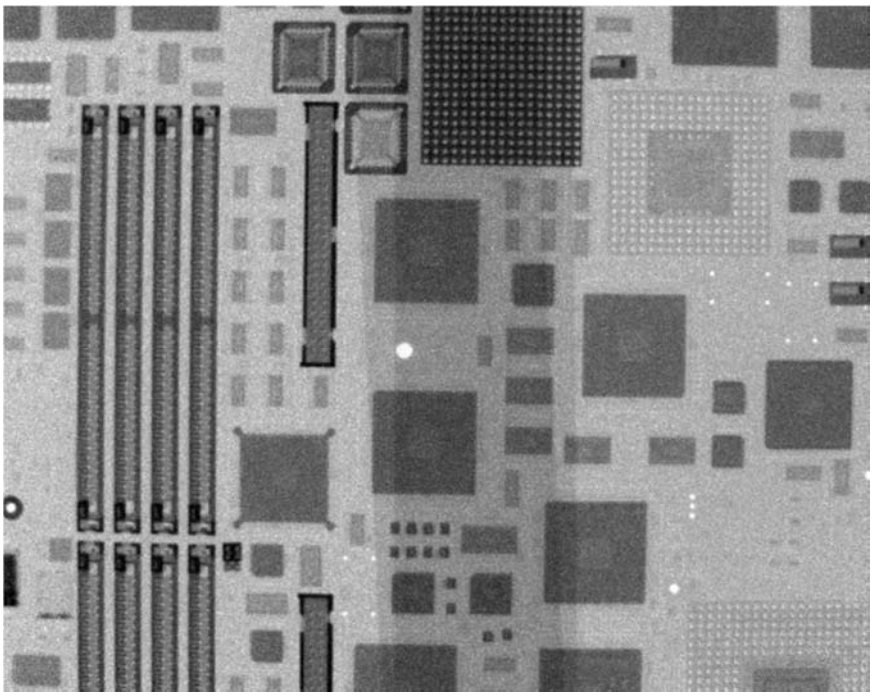

Neutron image.
Most contrast is given by plastic parts, the metal pins are nearly transparent.

## Comparison and combination of X-ray and neutron images

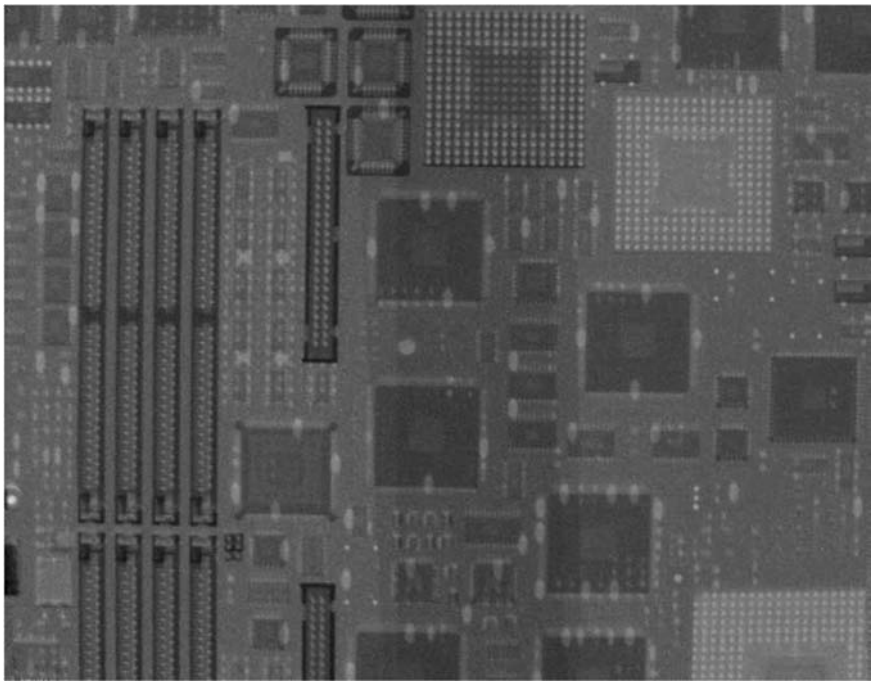

Combination of both images.
The X-ray image was subtracted from the neutron image.





## Comparison and combination of X-ray and neutron images

A toy plane combustion engine with a plastic propeller is another good example for the different properties of X-rays and neutrons.

The X-rays easily penetrate the plastic propeller, still penetrate the Aluminium well, but are heavily attenuated by steel parts.





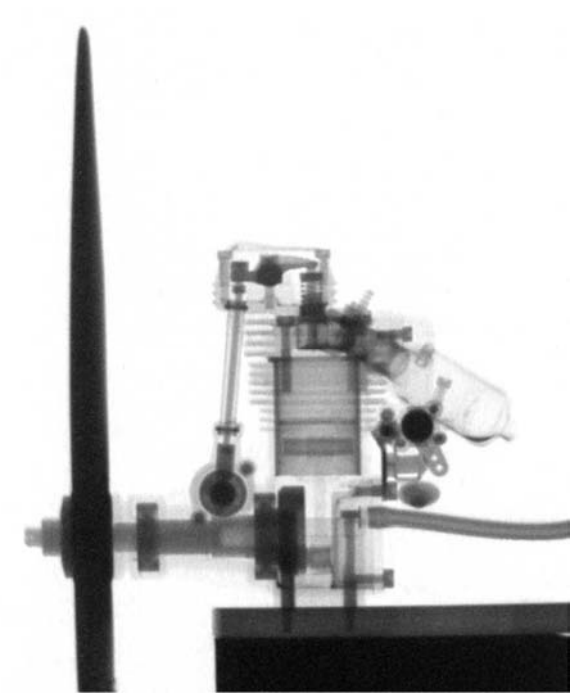

Aluminium is very transparent for neutrons, steel is better penetrated than by X-rays, but plastic is very opaque..

# Using liquid Gd contrast agent: Examination of water ingress into temperature sensors

NTC sensor in two-part plastic injection mold

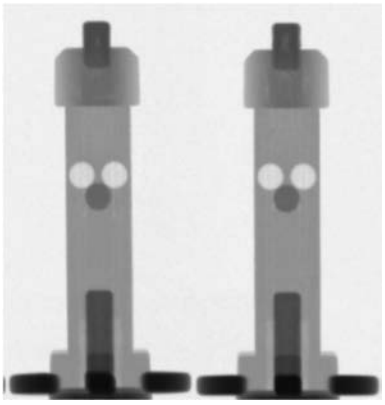

Inner injection mold

Outer injection mold added



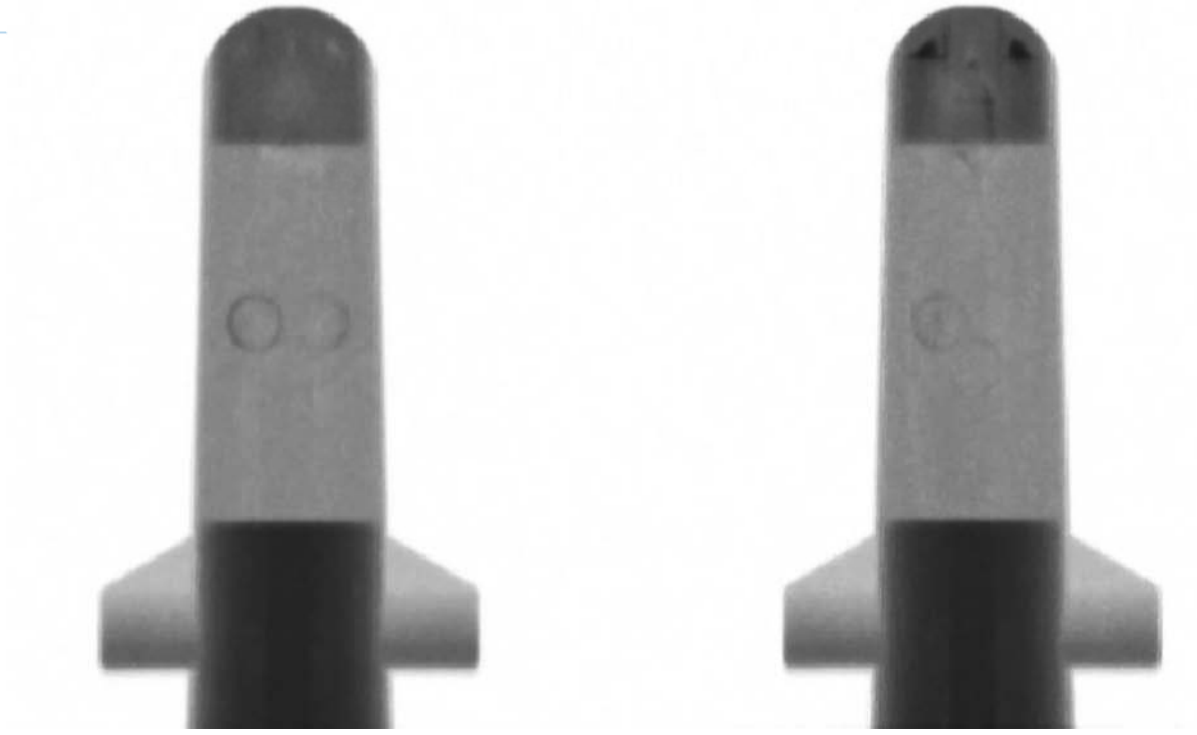

Sensors are put into a Gadolinium contrast agent, first evacuated, then pressurized to force the agent into cracks.

Sensors are put into a
Gadolinium contrast agent,
first evacuated,
then pressurized to force the
agent into cracks.





# Neutron tomography of highly heat loaded divertor components

The Wendelstein 7-X Fusion Experiment uses Plasma Divertors made of Carbon fibers and Copper plates to skim fusion products from the plasma and to extract energy.

Dues to very different thermal expansion coefficients, delamination occurs between the Carbon and Copper plates.

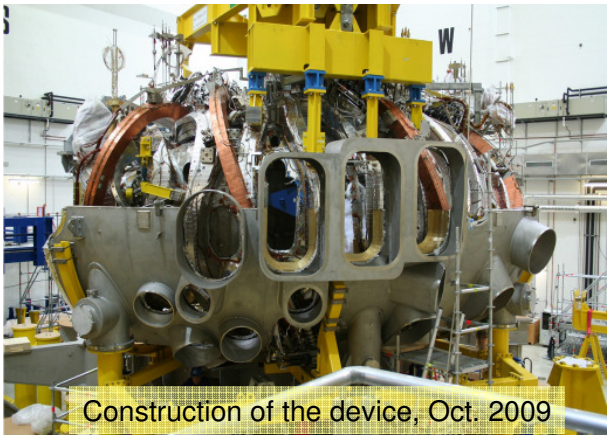


Construction of the device, Oct. 2009

# Design of divertor target

## Target element

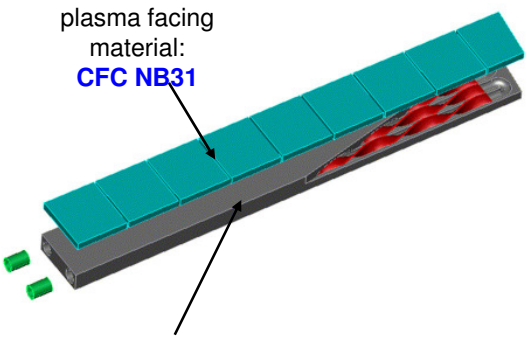


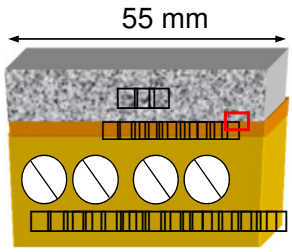


cross-section

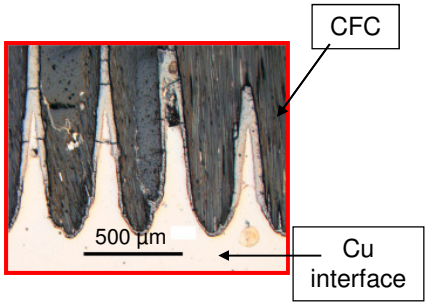


Magnification of CFC/ Cu interface





# Use liquid Gd contrast agent to fill the voids

**1. Submerse sample in liquid contrast agent**

**2. Evacuate space around liquid container:**

**Extract air from voids**

**3. Re-pressurize: External air pressure forces liquid into voids**

**4. Rinse in water**

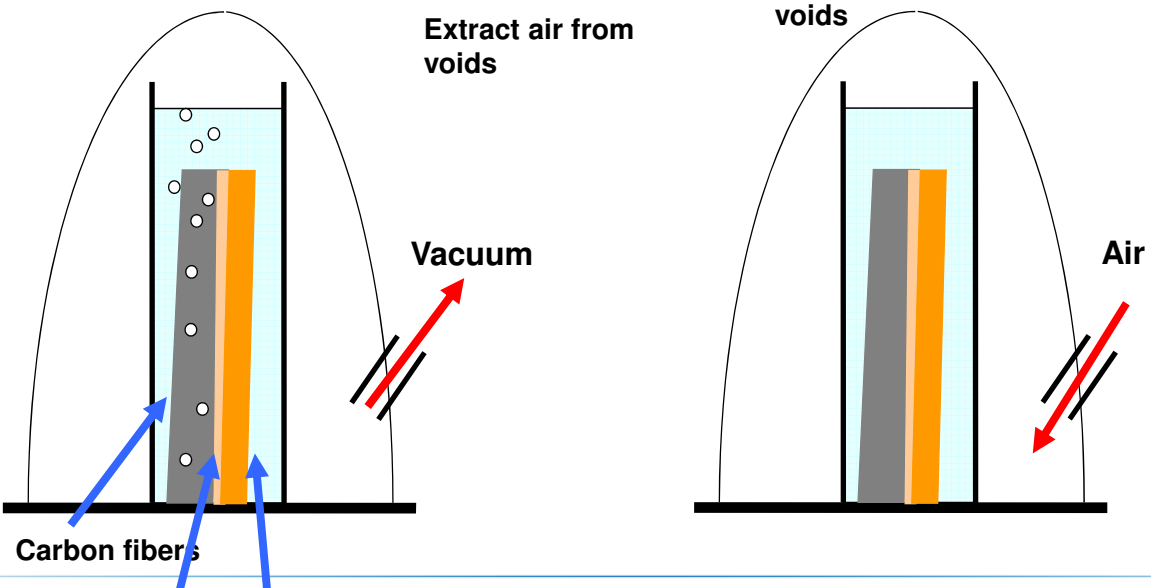

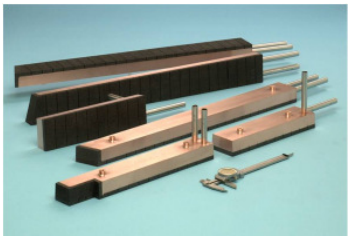

- Divertor function:
  - direct plasma contact
  - particle and power exhaust resulted in 10 MW/m² heat flux, $T_{surface}$ ~1000 °C

High heat flux tests performed in GLADIS (Garching Large Divertor Sample test facility)

The investigated component was loaded with 5000 cycles of 10 MW/m² and 10 s pulse length.

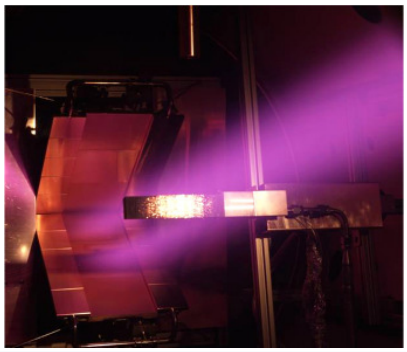





# Results of neutron tomography

**First 3D view: Cutout of plasma divertor, with Copper on top, Carbon below- the contrast agent fills the voids, also at the interface, and gives the brightest contrast.**

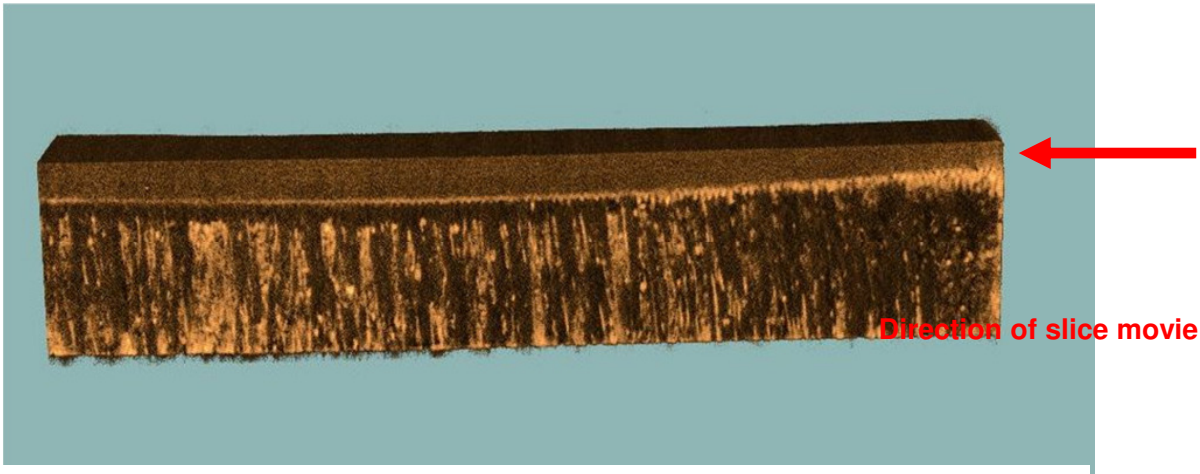


**The movie on the next slide walks through the tomographic slices, starting on the right side.**

**There is a heat loaded sample (left) and an unloaded sample (right).**

## Results of neutron tomography

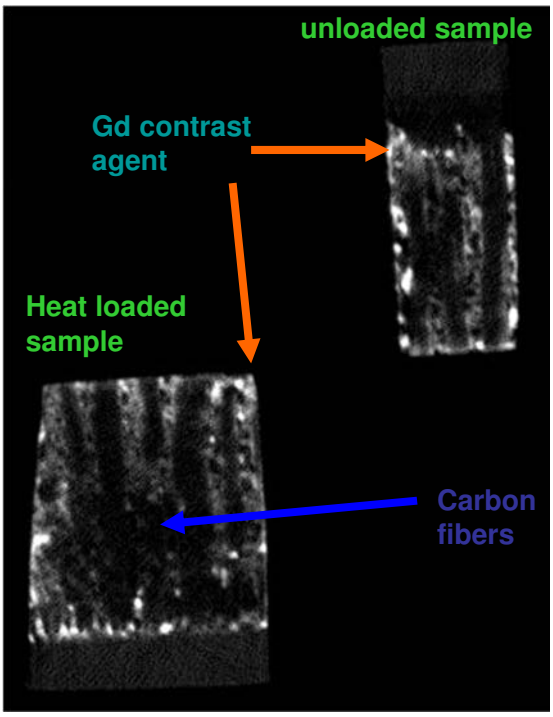


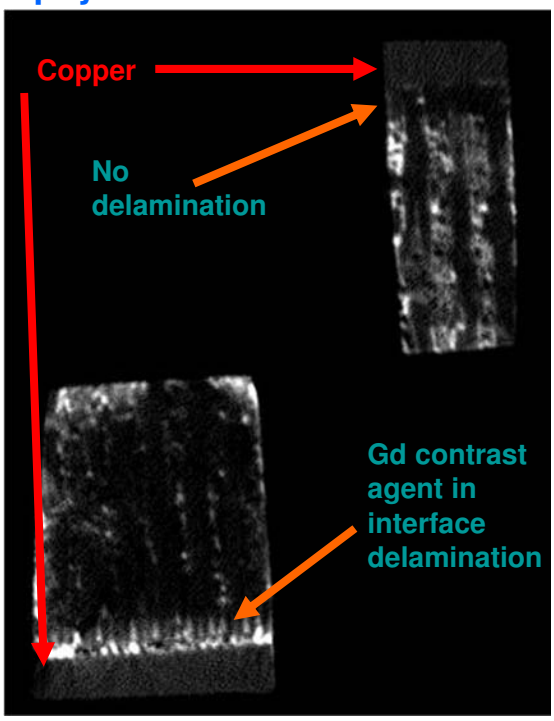






## Results of neutron tomography

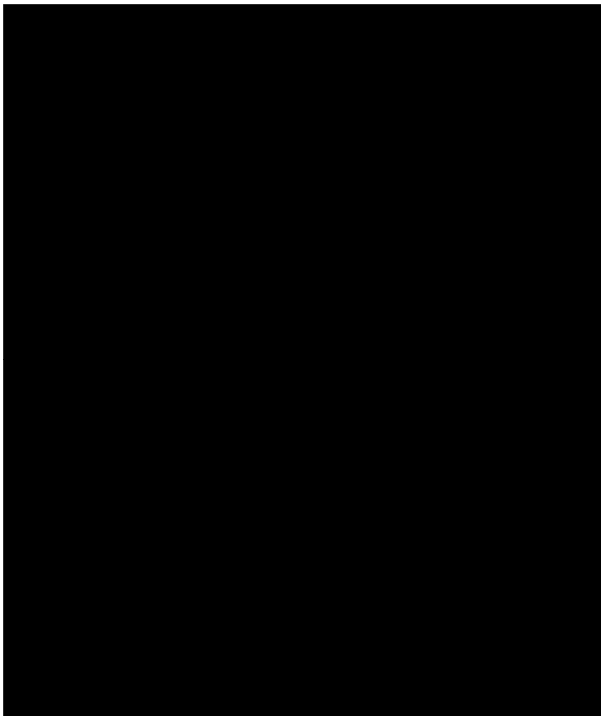

unloaded sample

Heat loaded sample

# Biomechanics: Pulmonary System

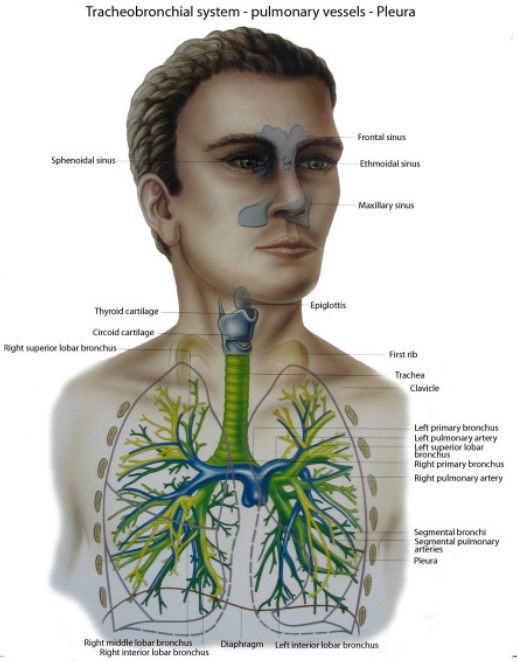


"**Terra Incognita**" with high potential clinical relevance

*Bridging the gap of different scales and physical areas*

Trachea
Ø 18mm

T. Bronchus
Ø 1.09

T. bronchiole
Ø 0.6

Alveoli
Ø 0.28
(Weibel 1963)

Fluid – Structure

Fluid – Liquid Lining – Structure

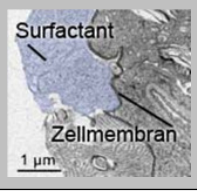






## Trachea

Generation: 1
Number: 1
Diameter: 18 mm
Area: 2.6 $cm^2$
Reynolds No.: 4350

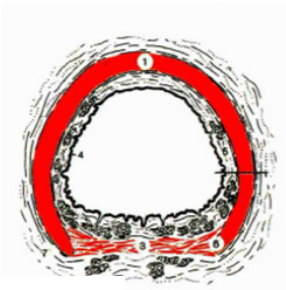

## T. Bronchus

Generation: 11
Number: 2050
Diameter: 1.09 mm
Area: 19 $cm^2$
Reynolds No. 34

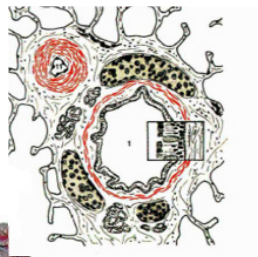

## Alveolar duct

Generation: 22
Number: 4.19 x $10^6$
Diameter: 0.41 mm
Area: 5900 $cm^2$
Reynolds No.: 0.04

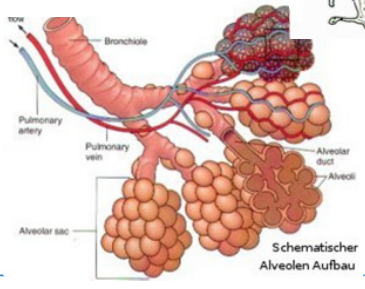


Weibel et al.

- **For the experiment, lungs are extracted from “recently deceased” rats.**
- **The lungs are confined in an Aluminium cylinder to simulate the ribcage**
- **They are inflated by 20-30 mbar air pressure**
- **For some lungs, 0.15 ml of a contrast agent containg Gadolinium were injected into the main air tube (windpipe)**
- **One lung was inflated without container**





## Neutron computed tomography on rat lungs

lung inflated inside
Al container

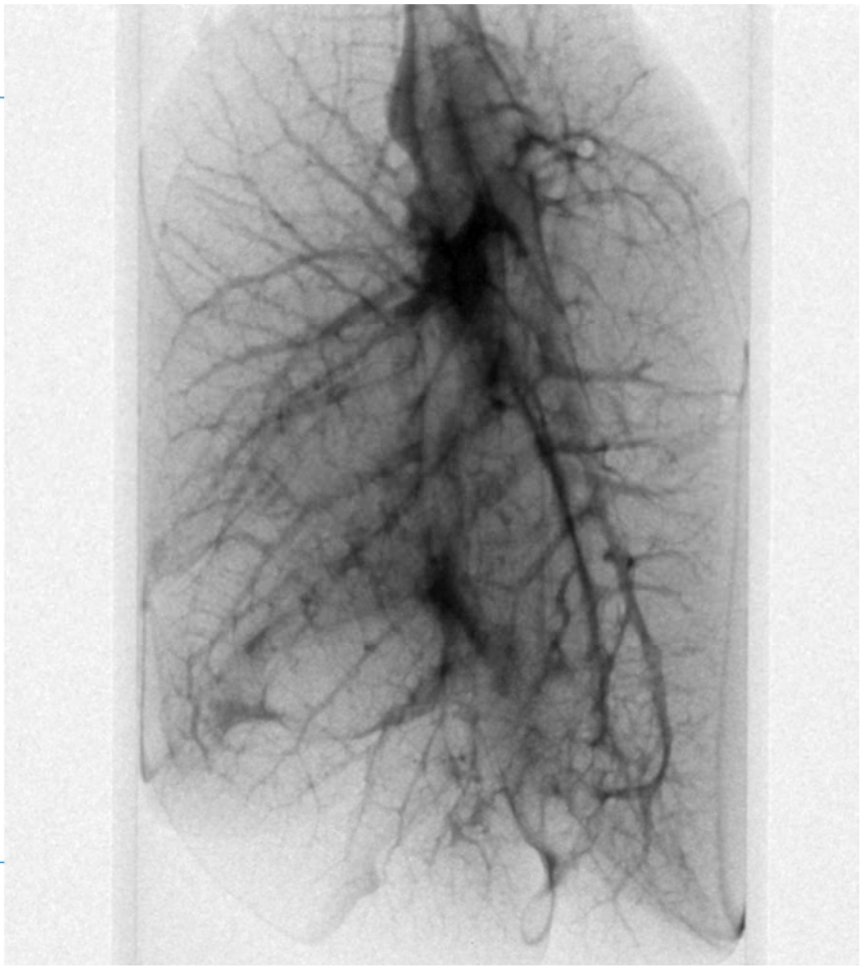

# Neutron computed tomography on rat lungs

lung fully inflated
without confining
container





# Neutron computed tomography on rat lungs

lung fully inflated
without container

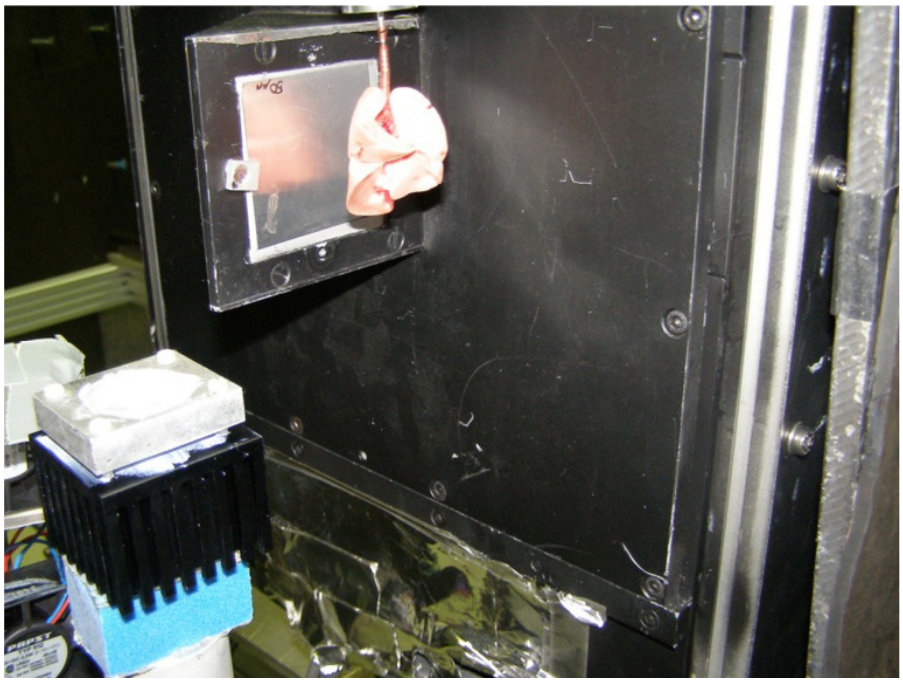

# Neutron computed tomography on rat lungs

lung fully inflated
in a non-confining
Container for the
CT scan



Demonstration of achievable resolution: Tomography of a rat lung of 4 cm size

Demonstration of achievable resolution:

Limit is in the order of 30 μm

Forschungsneutr
Heinz Maier-Leib

## Neutron computed tomography on rat lungs

Tomography of the lung with Gd contrast agent

# The limit is in the ZnS+$^6$LiF scintillation screen!

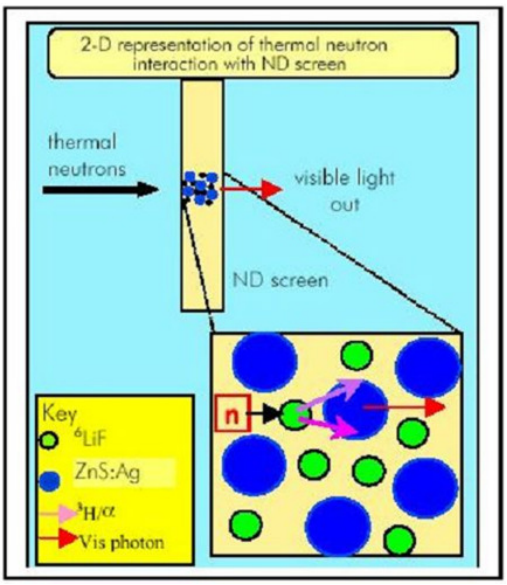


The reaction products of

$^6Li(n,\alpha)^3H + 4.7$ MeV

have to be stopped in the ZnS scintillation screen.
Their average range is in the order of 50-80 µm.

With thinned scintillation screens, we can achieve in the order of 20-30 µm.





# Measurements on a BMW engine at ANTARES, FRM-II

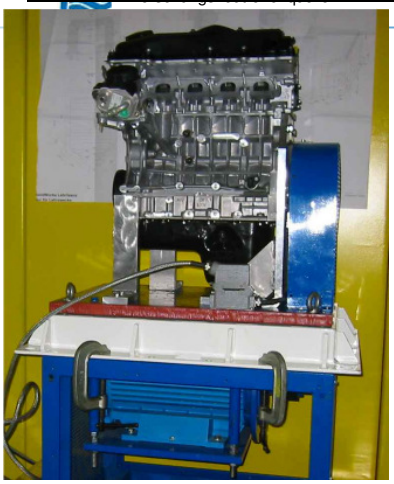

Static radiography of the engine,

with horizontal pressure tubes and vertical backflow tubes empty

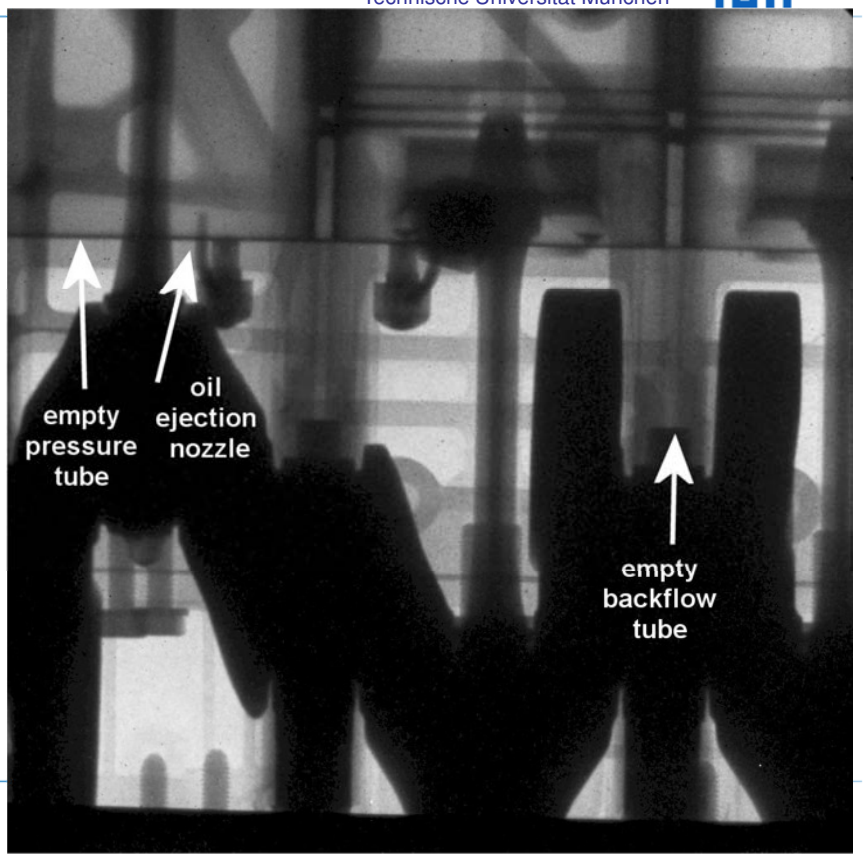

# Measurements at ANTARES, FRM-II



Dynamic radiography of the engine,

with oil filled horizontal pressure tubes and vertical backflow tubes,

and an oil blob within the oil jet to the piston bottom

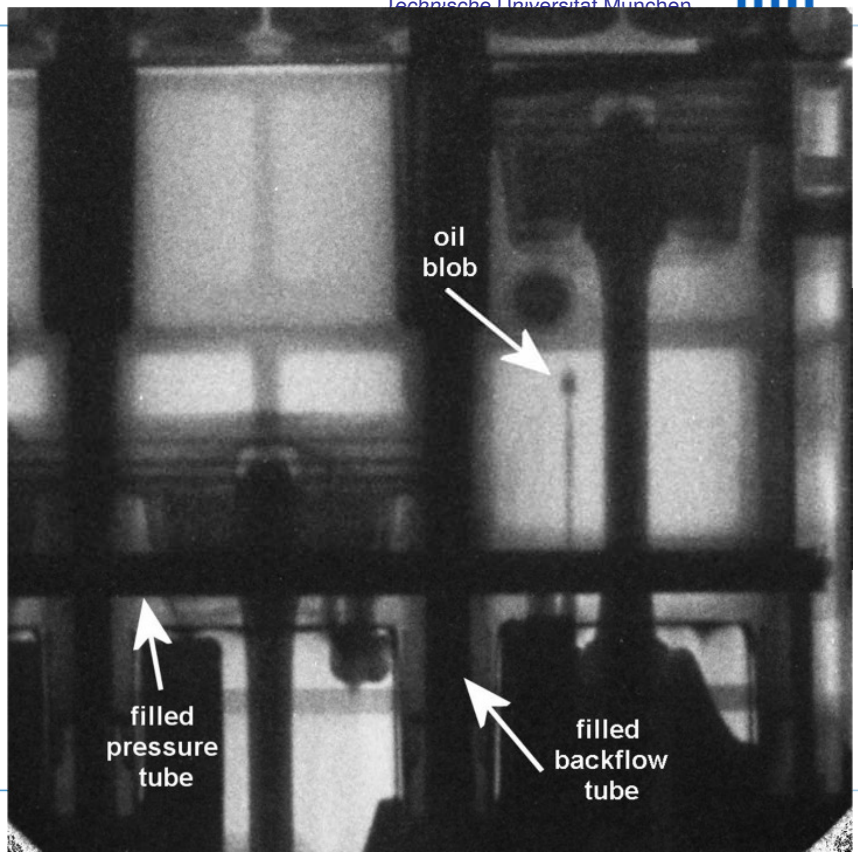






**Blobs in jet**

**Oil curtains detaching**

## Oil curtains detaching






# Detection of imprinted car chassis numbers in smooth-polished metal sheets

**E. Calzada, H. Li**
TU München FRM-II / Physik E21

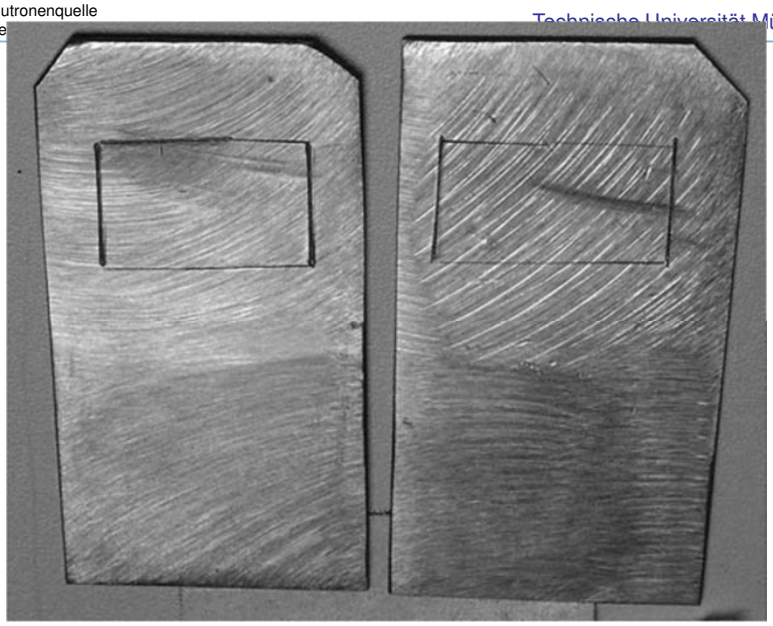

**The police brought us two smooth-polished metal sheets, where originally the car chassis numbers had been imprinted.**

**Nothing is visible on the surface, but deep in the metal, the structure has been altered…**





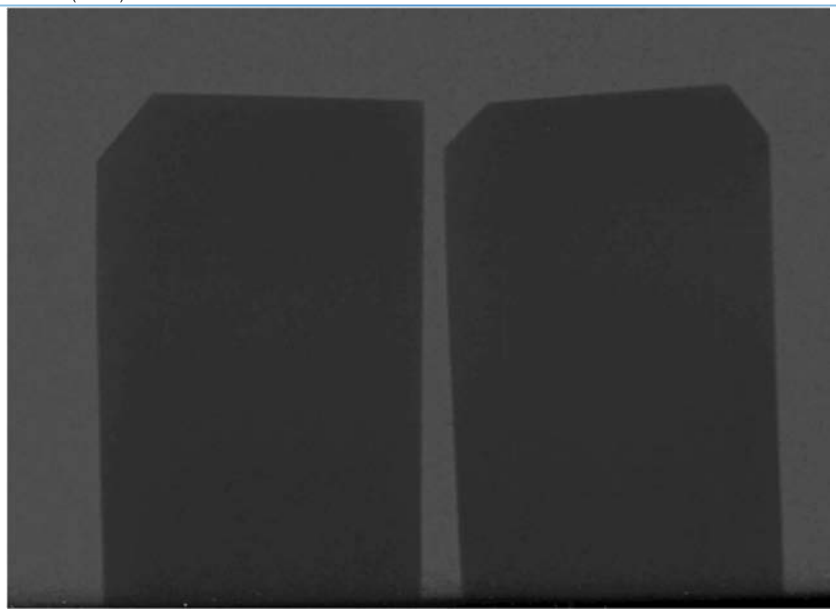

**The normal radiography shows nothing at all.**

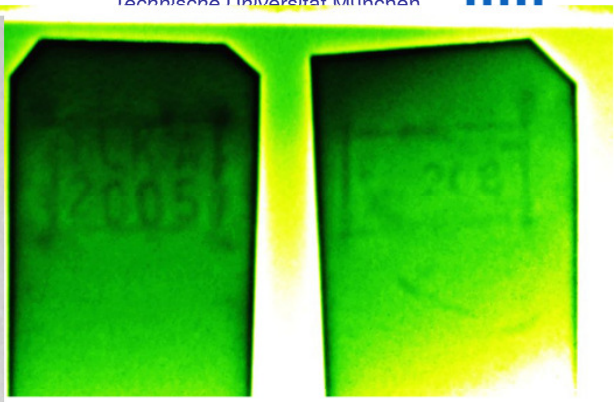

**But with a 7 mm pinhole, and 2 meters distance to the detector…**

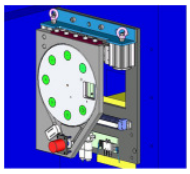





# *Neutron Imaging:*

## Detection of texture alteration in steel and Al parts using Small Angle Scattering in Neutron Radiography and Computed Tomography

**B. Schillinger, E. Calzada, M. Hofmann, H. Li**
TU München FRM-II and Physics E21

**A. Steuwer, R. Gähler**
Institut Laue-Langevin, Grenoble

**L. Edwards**
The Open University , Milton Keynes

# Reminder: Bragg's law

Coherent scattering on crystallites in materials:

$$n\lambda = 2d\sin\theta$$

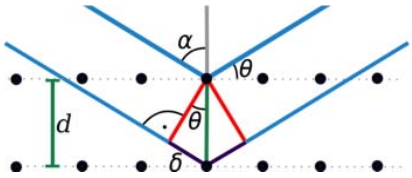


- scattered neutrons leave the direct transmitted beam path and cause attenuation in the transmission image
- The maximum scattered wavelength is $\lambda = 2d$
- no coherent scattering for $\lambda > 2d$
- higher transmission for $\lambda > 2d$
- depending on texture changes: varying transmission





# Cold expanded fastener holes


- The primary source of aircraft fatigue is at joints.
- Cold expansion increases joint durability.
- Quantification of the benefits of cold expansion requires accurate reliable residual stress estimation.

# The cold expansion process

- The most common method is FTI split sleeve expansion.
- At present, air worthiness authorities do not allow the benefits of cold expansion to be included in design calculations.

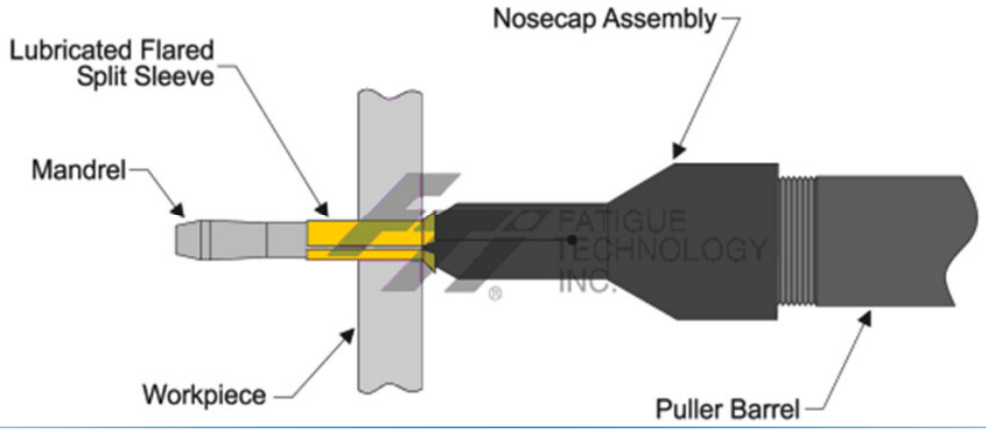


***Picture**:http://www.fatiguetech.com/products/splitsleeve.html*





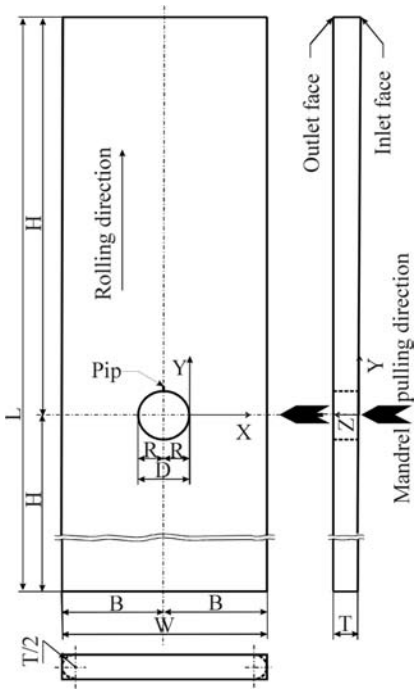


**Test sample:**

Aluminium sheet

Rolled out along the longitudinal direction

180 mm length, 40 mm width, 5 mm thickness

Initial hole drilled with diameter 9.52mm (3/8inch)

Cold expansion (4%) to 10 mm diameter

Strain measurements with synchrotron radiation, neutrons, and simulated data

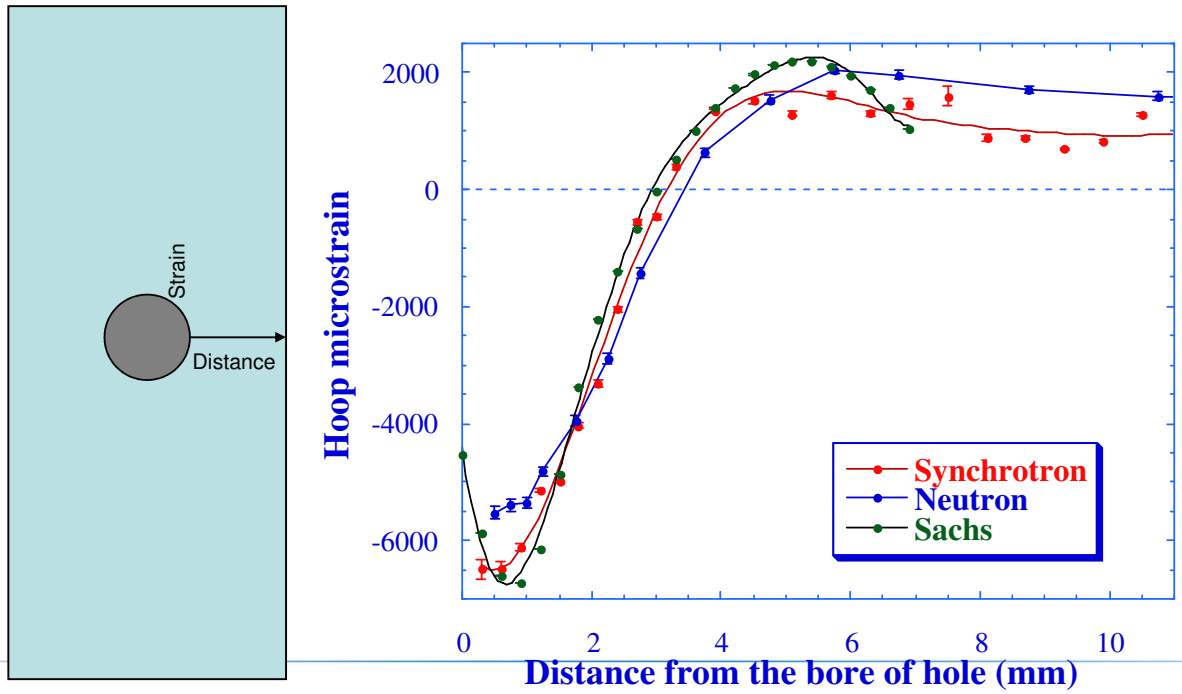




# Measurement of a 3D computed tomography of the test sample

• Distance sample to detector was approx. 50 cms.

• 400 projections recorded for calculation of the tomography

• The tomography delivers a range interval of gray values for the attenuation of Aluminium

• For visualisation of the 3D tomography, nearly the whole attenuation range for Aluminium is set transparent, only the most attenuating part is set visible.

•The expanded area at the hole rim produces increased scattering,
which in turn leads to increased attenuation of the transmitted beam.
The area clearly shows up in the computed tomography.

•Surprise: Even a wave structure resulting from the rolling of the Aluminium sheet is visible!

Piece of tape

Pieces of glue

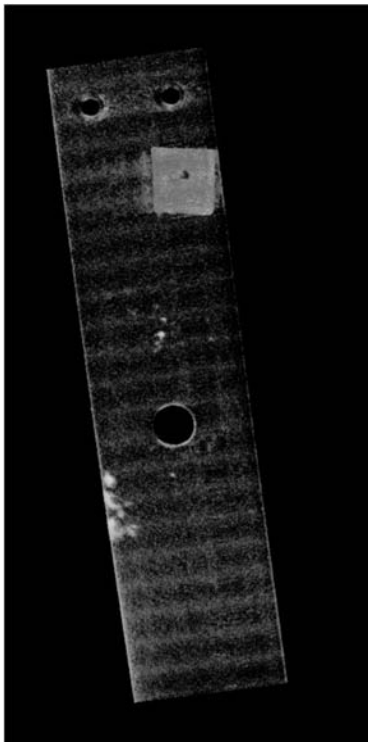

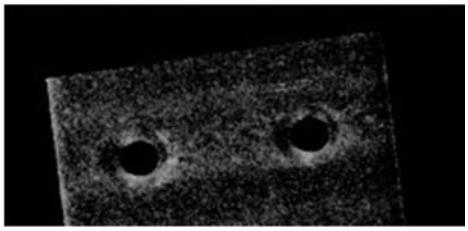

Ordinary holes with phased edges

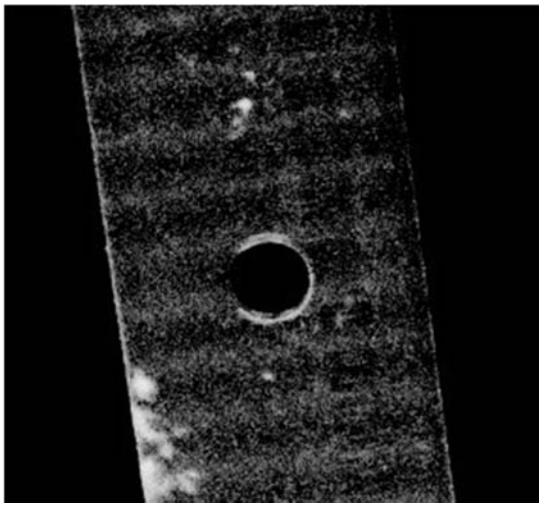

Widened hole compressed Edges.

The widening was asymmetric.

Surprise: Even a wave structure resulting from the rolling of the Aluminium sheet is visible!

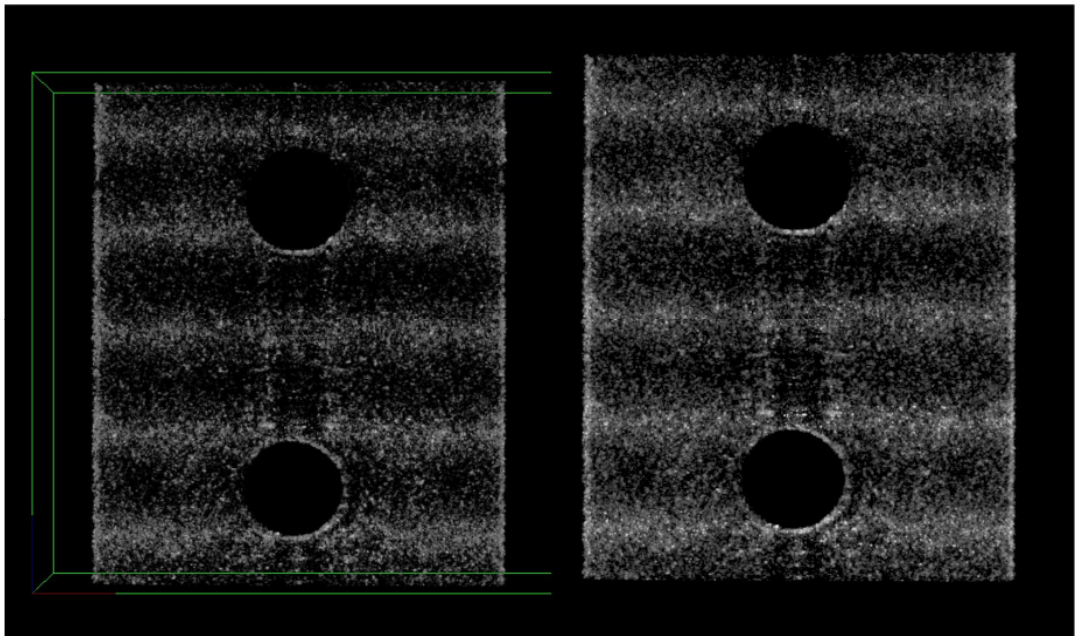

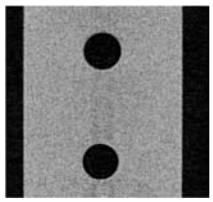

Above: Normal full view of the piece.

Second hole drilled for second tomography.

This was recorded with a smaller detector with less dynamics and sensitivity.
The distance to the detector was only 25 cms, but still, the difference is clearly visible!

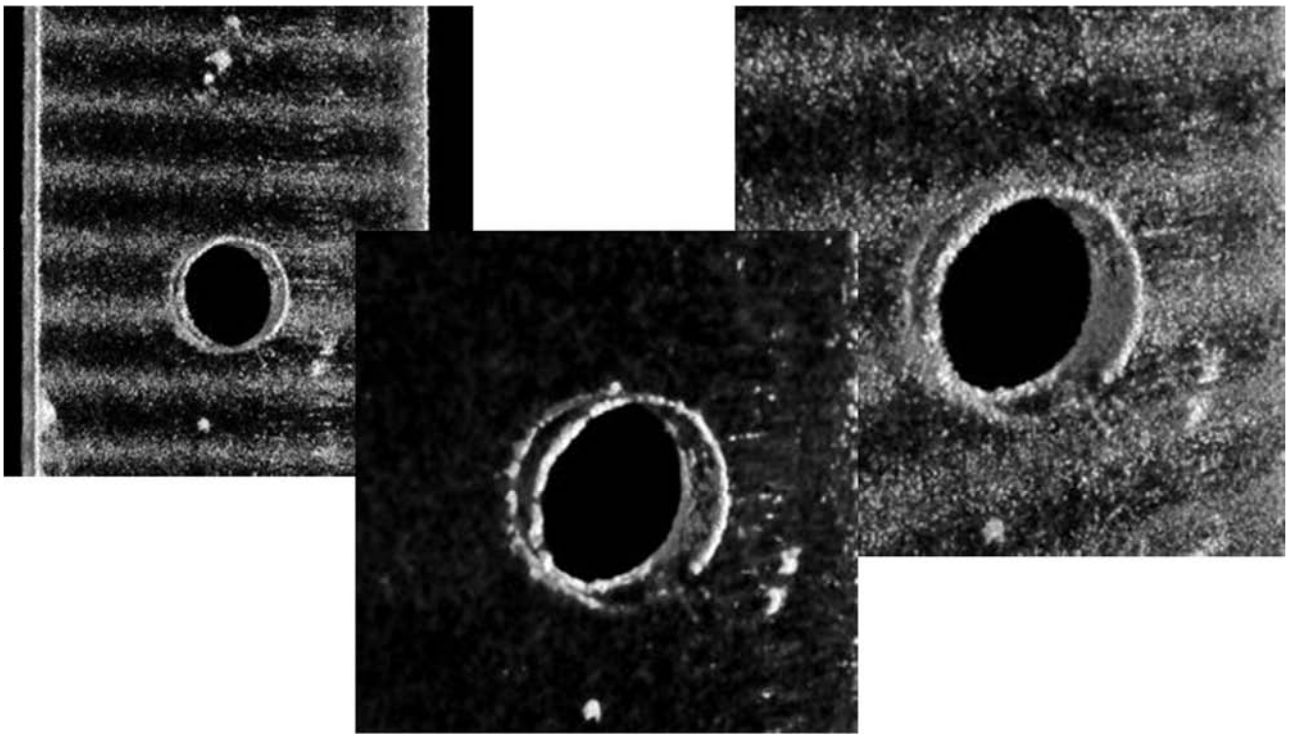

These pictures show more clearly that they represent a true 3D tomography.

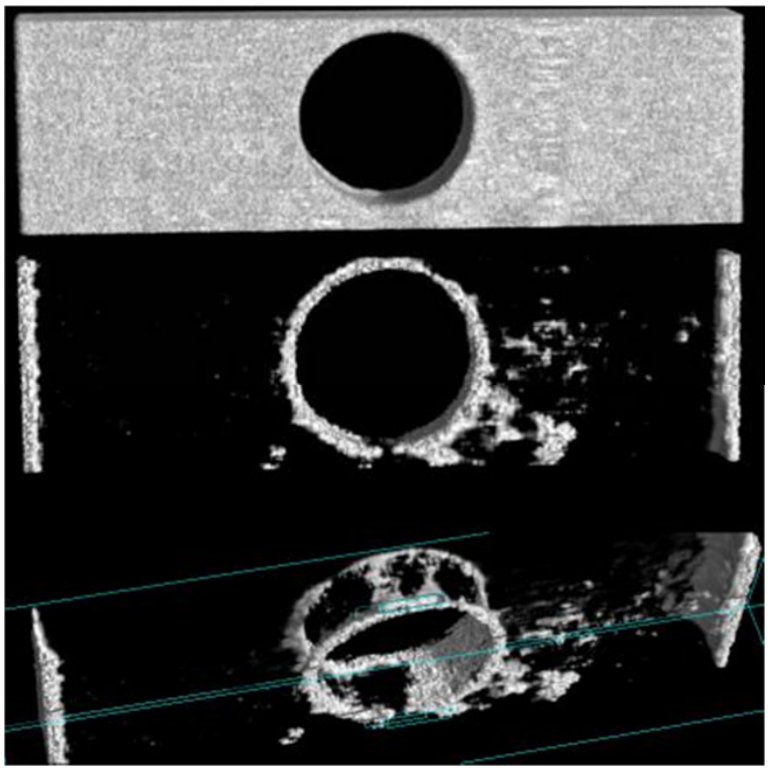

The edge of deformed material segmented in 3D.

# Phase Contrast Radiography with X-Rays and Synchrotron Light

X-ray image of a genetically engineered mouse (source: www.xrt.com.au):

Conventional radiography

Phase contrast radiography





# Refraction of a wave by a medium

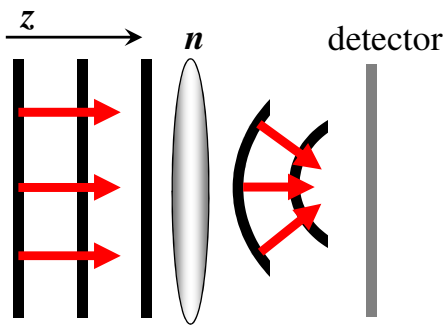


Refractive index:

$$n = 1 - \delta - i\beta$$

phase shift: $\delta$ — absorption: $i\beta$

Angular deviation of the normal: $\Delta\alpha \propto \lambda \left| \nabla_\perp \varphi \right|$

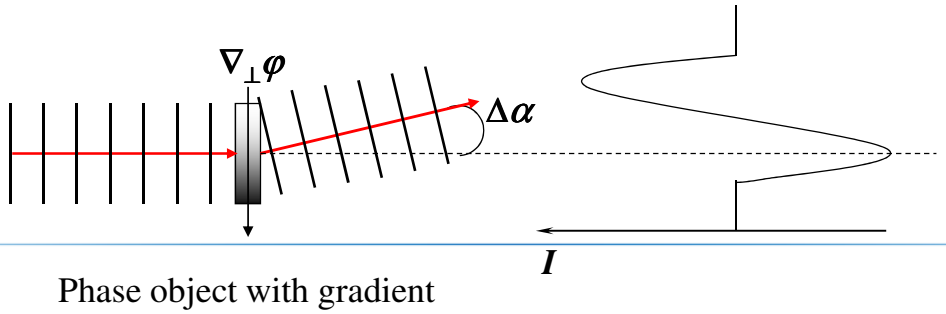


Phase object with gradient

# Requirements for Phase Contrast

1. Neutron beam with a high lateral spatial coherence length.

2. The detector plane must be in the near field region.

Schematic of a phase contrast radiography setup:

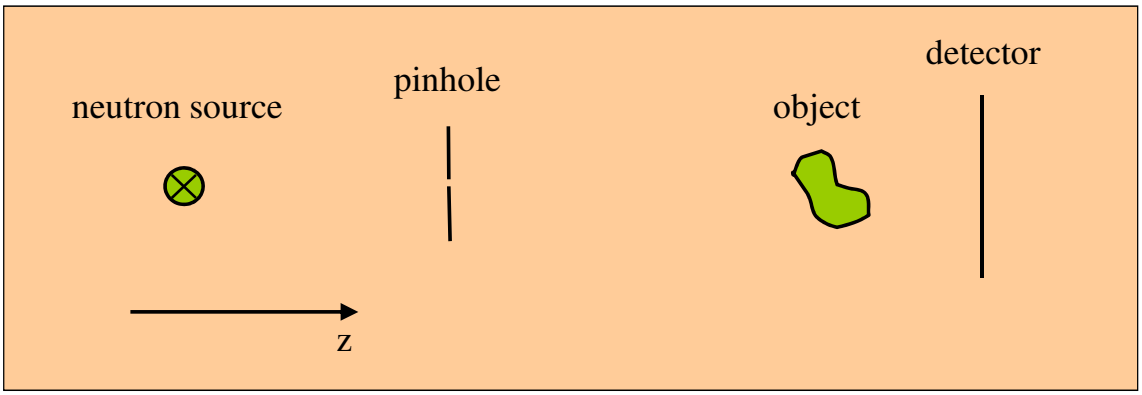


The small pinhole results in low intensity and large exposure times!
(several minutes to hours per radiograph)





# Investigations on metal foams

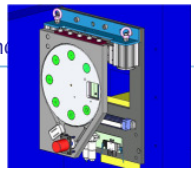

information about the average bubble size,
standard deviation, homogeneity of the distribution of the bubbles

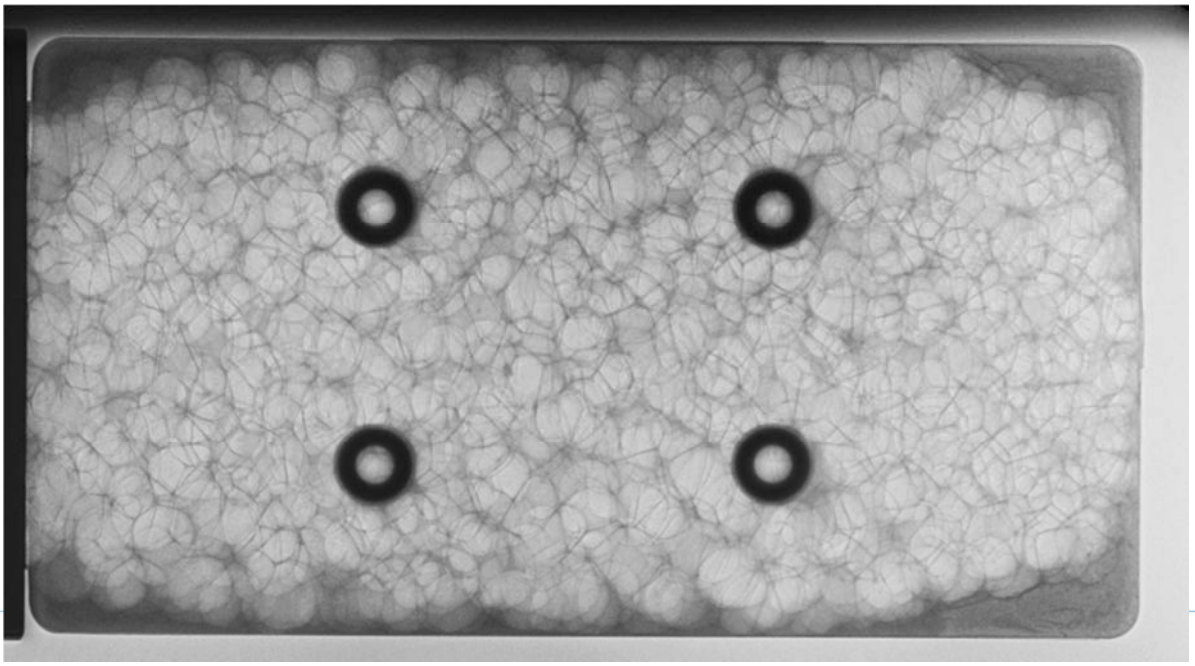

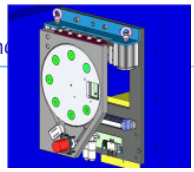

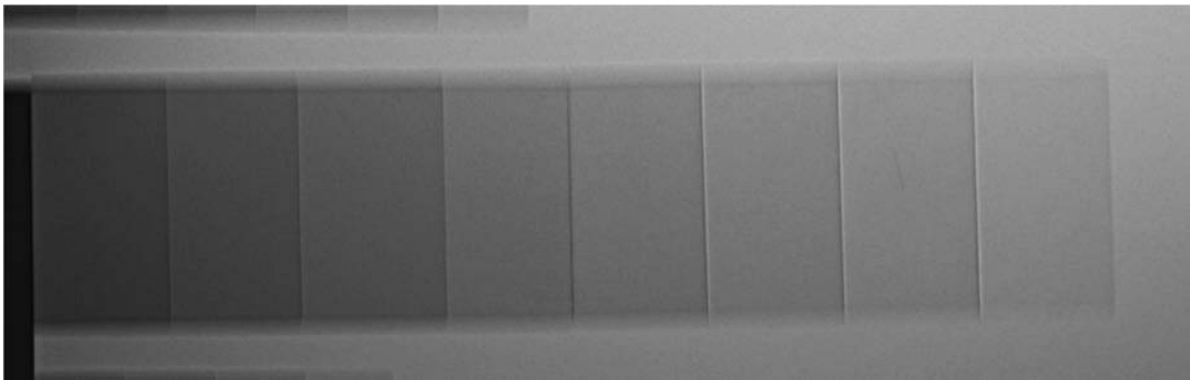

On a massive step wedge, we can even see
the bright and dark part of the edge enhancement!





**Step wedge made from one Aluminium alloy, with surrounding casting of a different Aluminium alloy with different index of refraction.**

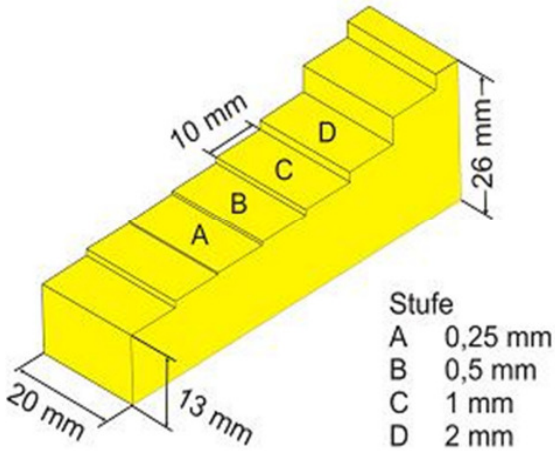


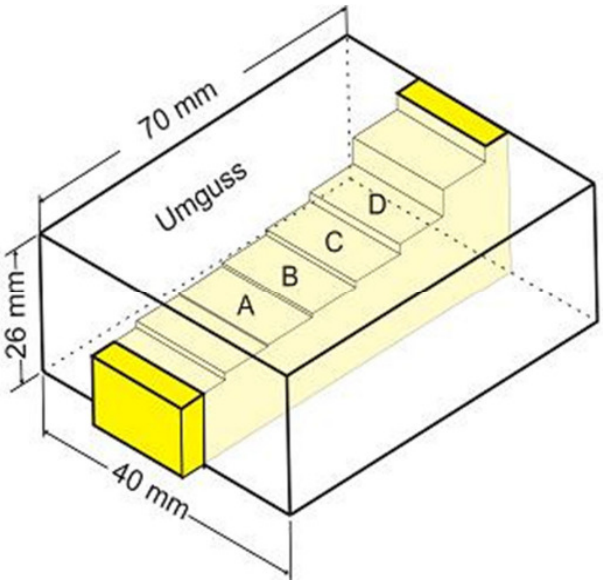

**Aluminium foam and step wedge with surrounding.**

**The standard radiograph (left) shows only air gaps, the phase contrast radiograph shows the material interface!**

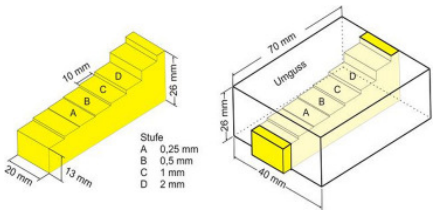


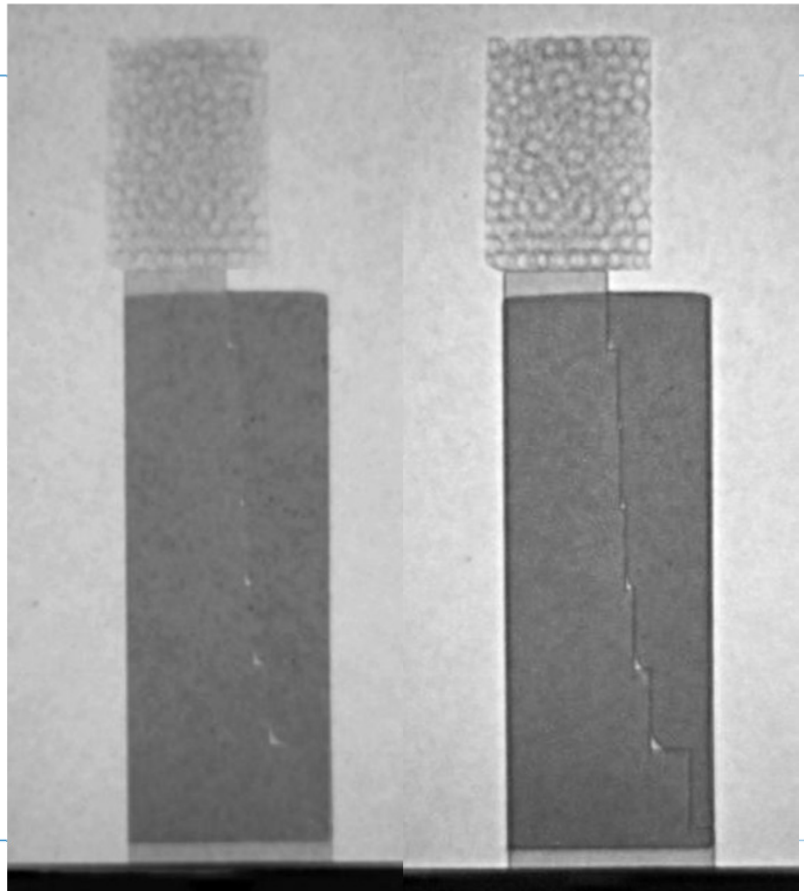





**90° rotated view:**
**The standard radiograph (left) shows no difference between the Aluminium alloys, the phase contrast radiograph shows the material interface!**

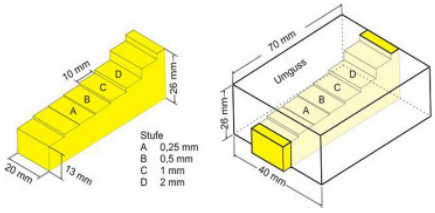


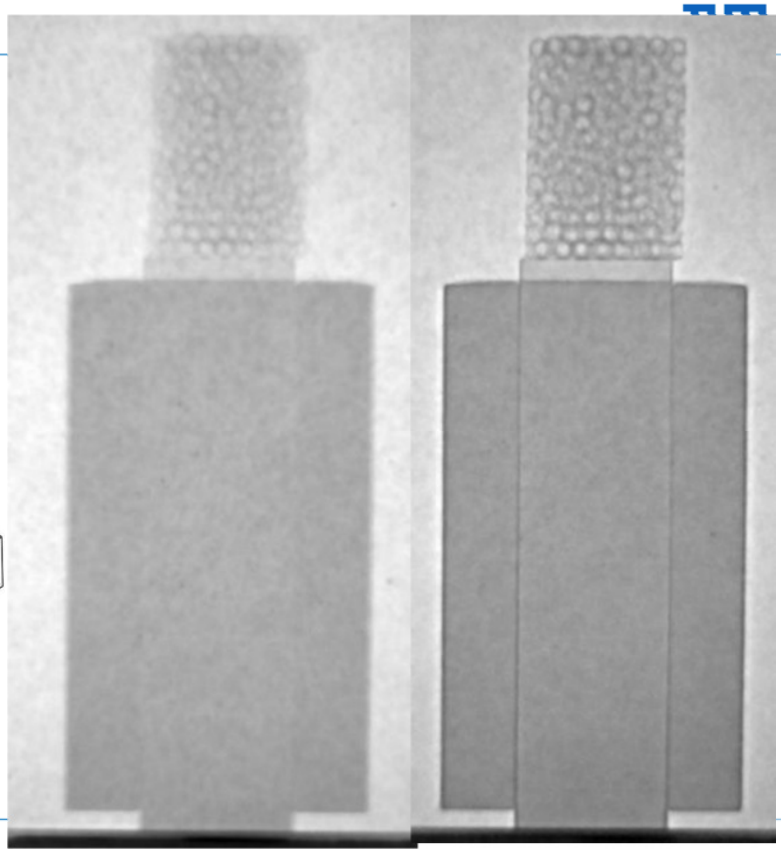

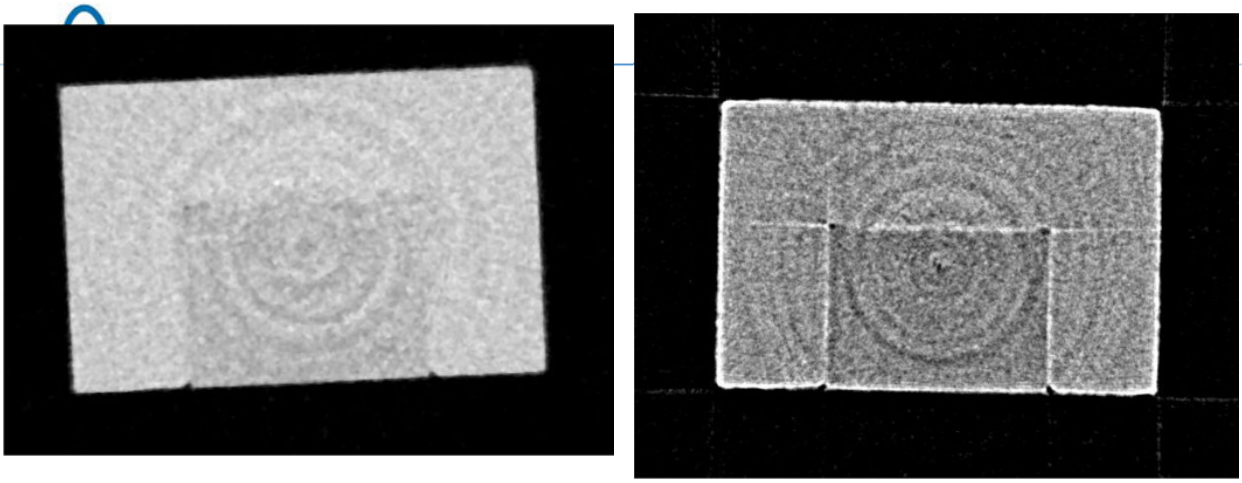

**Aluminium step wedge with surrounding casting**

**Left:** **Standard Tomography**

**Nearly identical attenuation for both alloys**

**Right:** **Phase contrast tomography**

**Strong edge enhancement but new reconstruction artefacts!**





# Energy dependent neutron imaging with a double crystal monochromator

Michael Schulz, Peter Böni, Elbio Calzada, Klaus Lorenz,
Martin Mühlbauer, Burkhard Schillinger
FRM-II and Physics E21, Technische Universität München

# Why monochromatic neutron imaging?

- No beam hardening
  - Quantification of material thicknesses
- Scattering and absorption energy dependent
  - Energy dependent effects can be used to characterise materials
- Higher possible sample thickness
- Bragg edge location

  - Detection of materials

  - Discrimination of different material phases





# The double crystal monochromator

Wavelength selection by Bragg's Law:

$$n\lambda = 2d\sin\theta$$

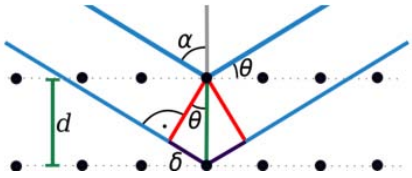


- Two pyrolytic graphite (002) monchromator crystals (size: 6x10cm², Mosaic spread approx. 0.7°)
- Crystals can be rotated and one can be translated along beam direction
- By zig-zag reflection outgoing beam has same direction as incoming beam but is shifted by 105 mm

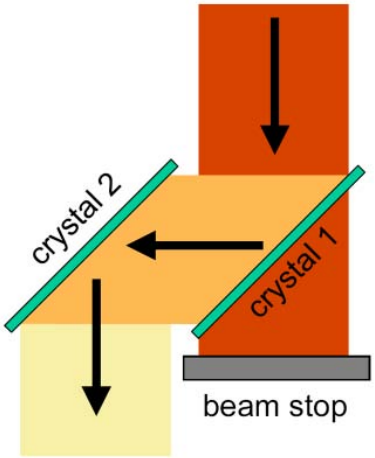

# Details

- First crystal can be moved out of beam  no attenuation of polychromatic beam
- Flight tube is big enough to contain the shifted beam
- High L/D, since monochromator is mounted close to pinhole aperture
- Wavelength range: 2.7 Å  6.5 Å
- Sharp wavelength selection:  1% <  < 4%
- Monochromatic beam size at detector position: approx. 20x20cm²
- Homogeneous intensity over FOV
- Intensity approx. 200 times lower than polychromatic beam
- Typical exposure times: 5min per radiograph

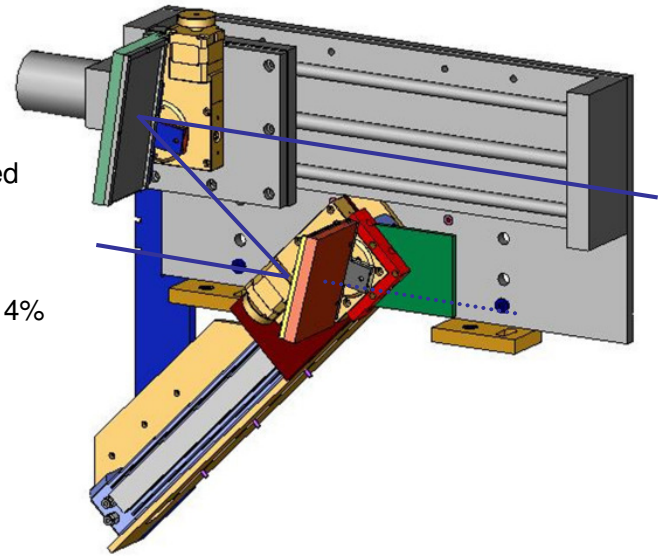





# Measurements

- Intensity
- Friction Stir Welds
- Different phases in conventional welds

# Intensity

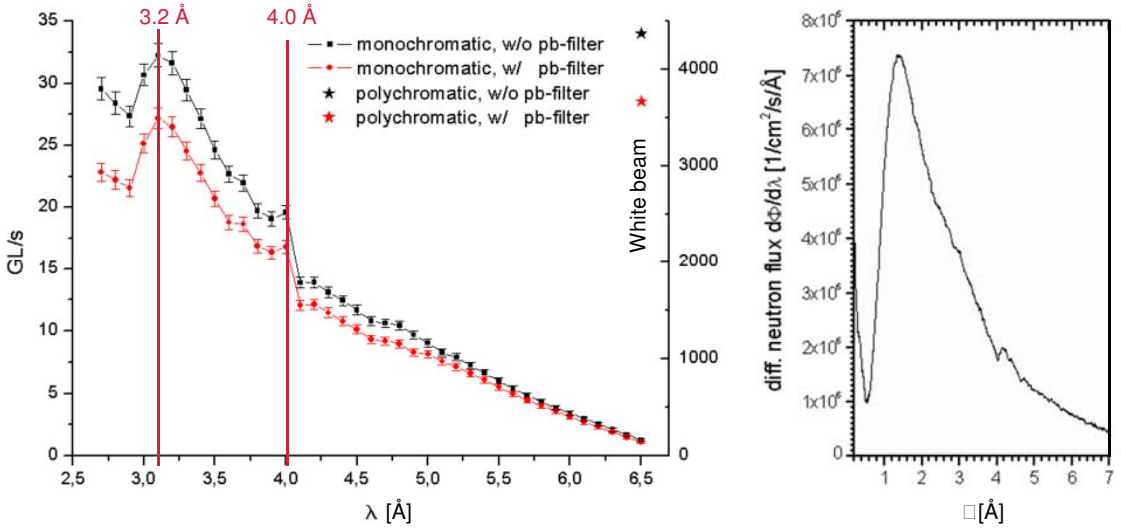


- Monochromatic intensity is at least a factor 130 less than polychromatic flux
- Approx. linear decrease of intensity with wavelength





# Friction Stir Welding

a solid state joining process

shoulder

pin

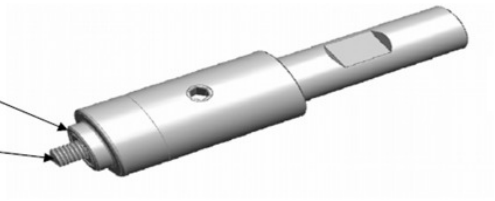

FSW-Tool

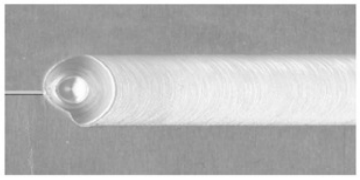

FSW working principle

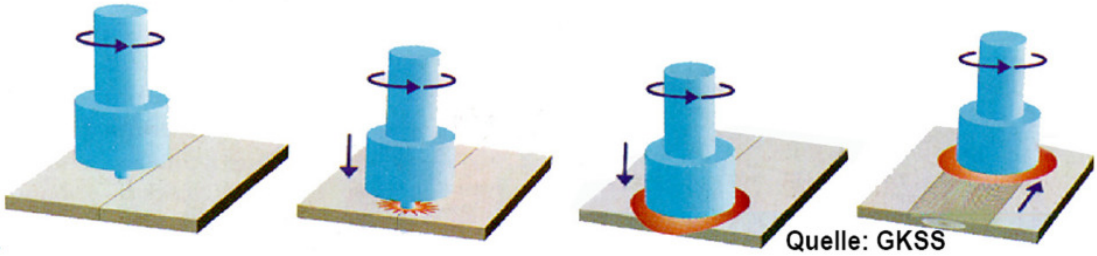

# Reminder again: Bragg's law

Coherent scattering on crystallites in materials:

$$n\lambda = 2d\sin\theta$$

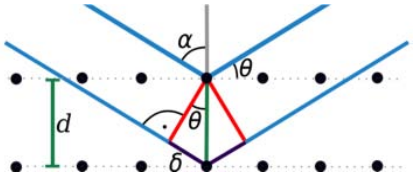


- scattered neutrons leave the direct transmitted beam path and cause attenuation in the transmission image
- The maximum scattered wavelength is λ = 2d
- no coherent scattering for λ > 2d
- higher transmission for λ > 2d
- depending on texture changes: varying transmission





# Friction Stir Welds

- Bragg Edge of Al is at 4.7 Å
- Wavelength dependent attenuation was measured from 2.7 Å to 6.0 Å
- Low attenuation of Al leads to long exposure times of 45 min to give sufficient contrast
- Texture: preferred orientation of crystallites wrt. the incoming beam leads to dark areas at certain wavelengths
- Each wavelength corresponds to one reflection angle

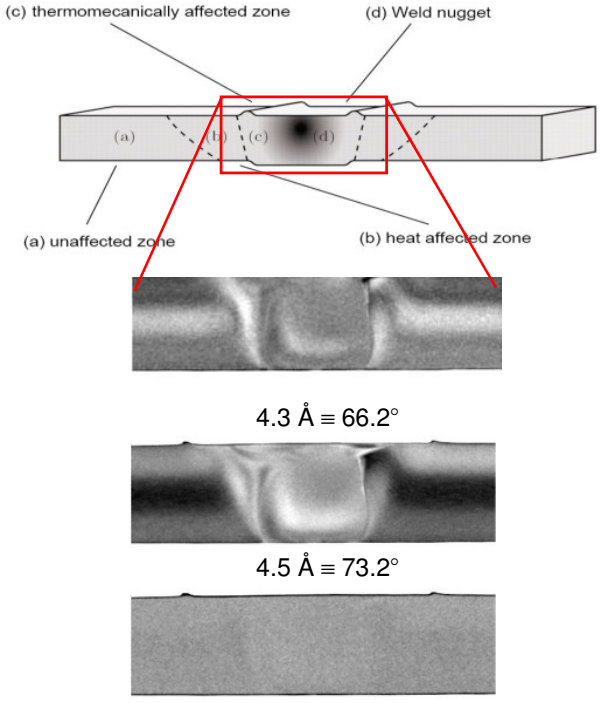

# Energy scan of Friction Stir Weld

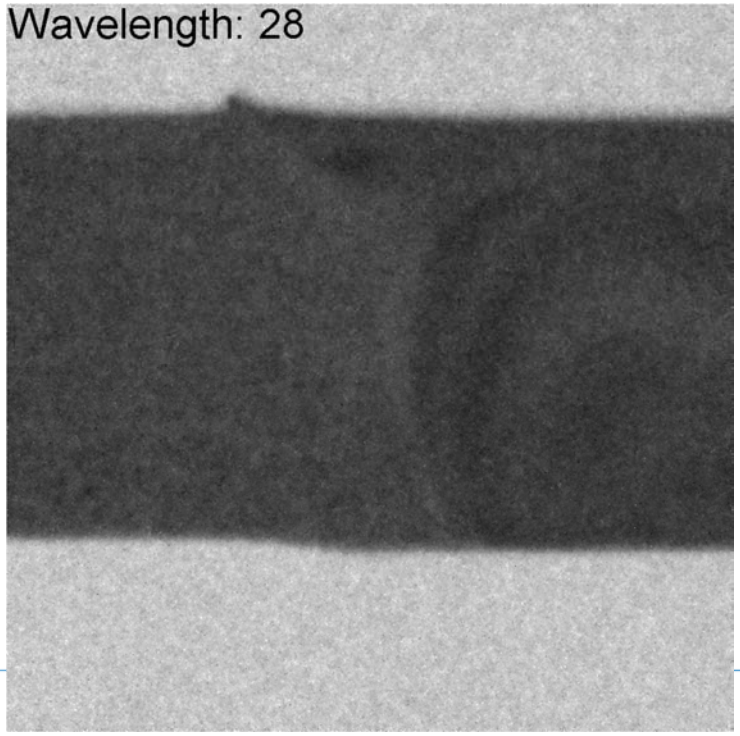






# Macroscopic dark field imaging using scatter grids

Burkhard Schillinger
Forschungsneutronenquelle Heinz Maier-Leibnitz (FRM II)
Technische Universität München

# Neutron radiography

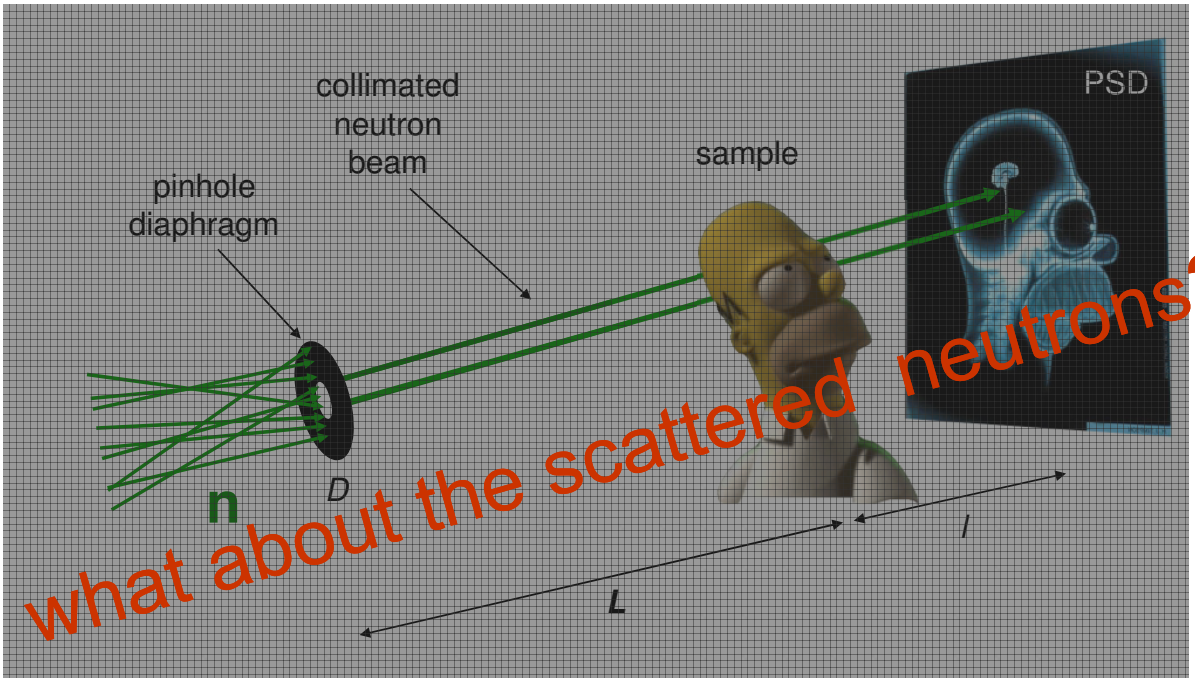


F. Piegsa, PSI





# Initial Motivation: Directly measure the scattered neutron contribution in standard radiography

- Neutron radiography treats both absorption and scattering as attenuation.
- It is assumed that scattered neutrons do not reach the detector.
- When the sample is close to the detector, scattered neutrons cause a diffuse background, which adds to the exponentially attenuated signal.

# Experiment:

Two absorbing grids block the direct neutron beam

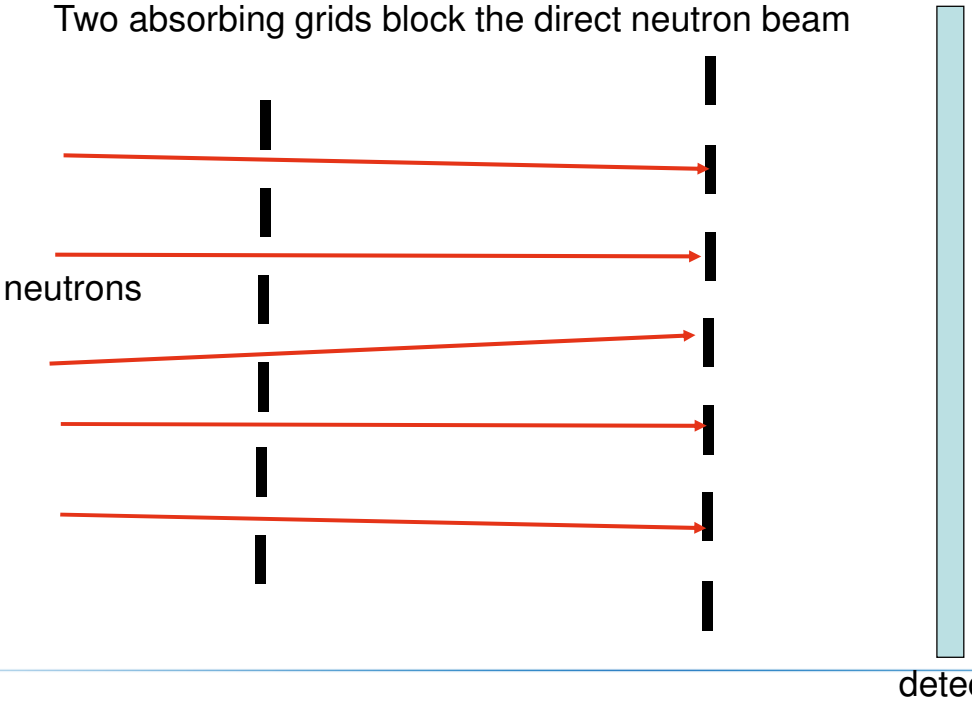






# Experiment:

Two absorbing grids block the direct neutron beam

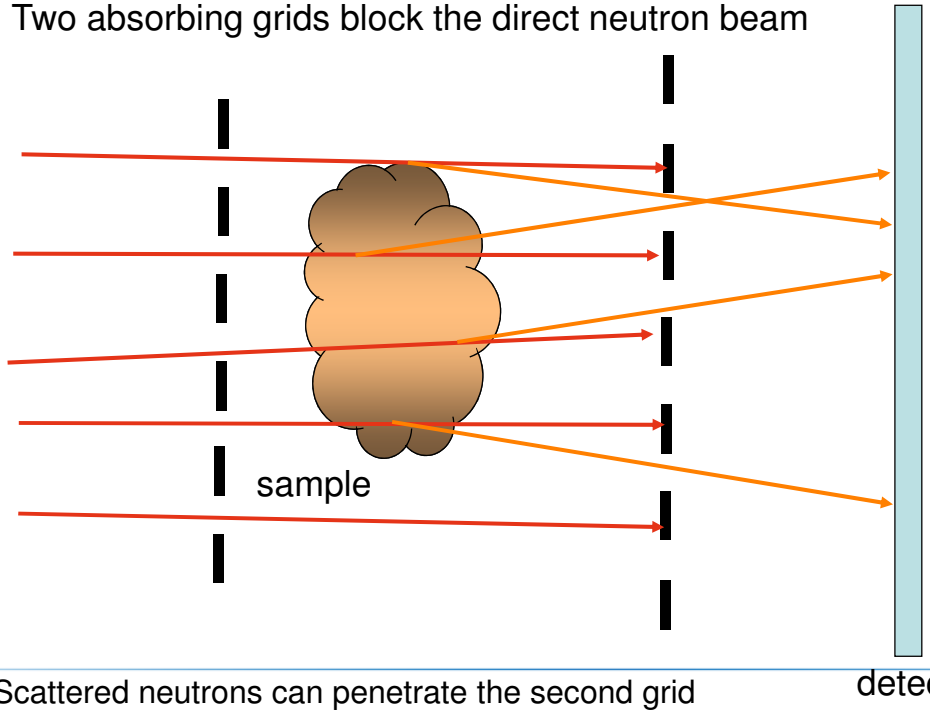


Scattered neutrons can penetrate the second grid and reach the detector.

# Experiment:

First setup:
Two Cd grids with
1mm gap and
1.2 mm bar

As Cadmium is transparent for neutrons with E>0.4 eV,
a Beryllium filter was used,
transmitting only neutrons
with E<0.004 eV (4 Angström).

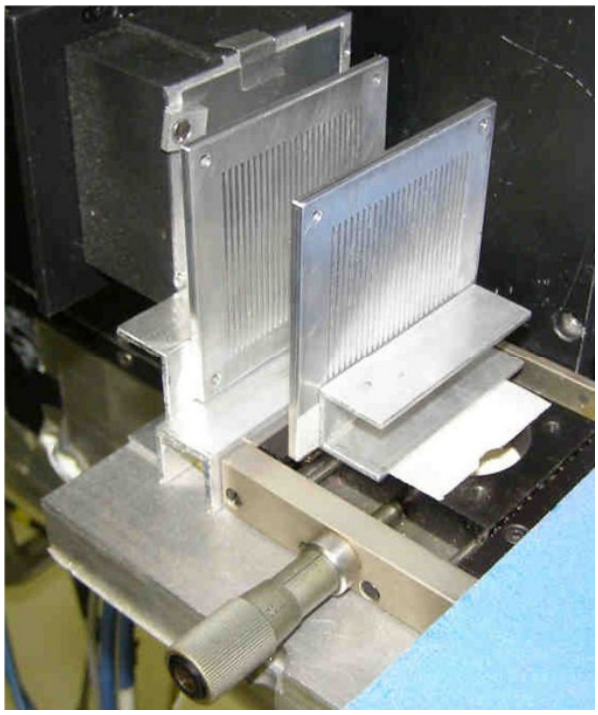





# Experiment:

2nd setup:
Two Cd grids with
1mm gap and
1.2 mm bar

Rubber stopper with
steel screw and
stainless steel nut,

stainless steel screw,

and steel screw.

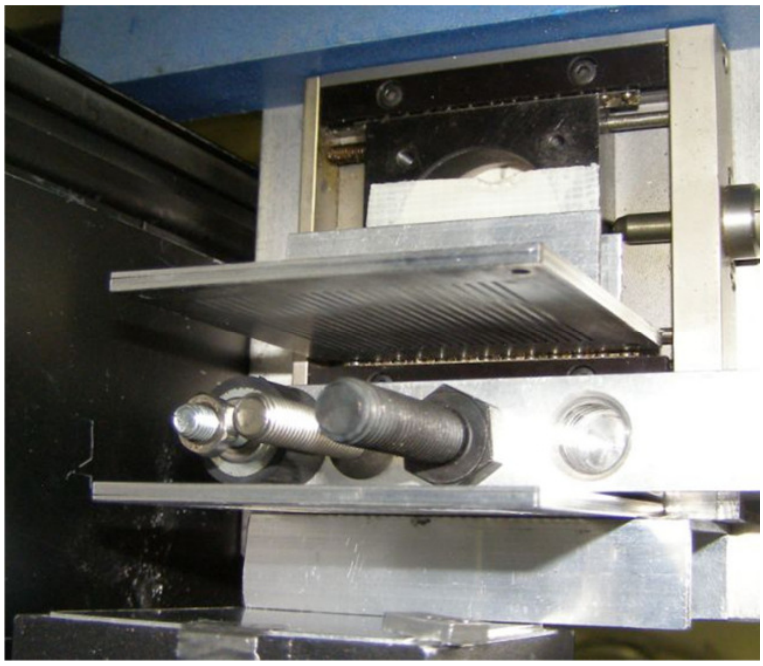

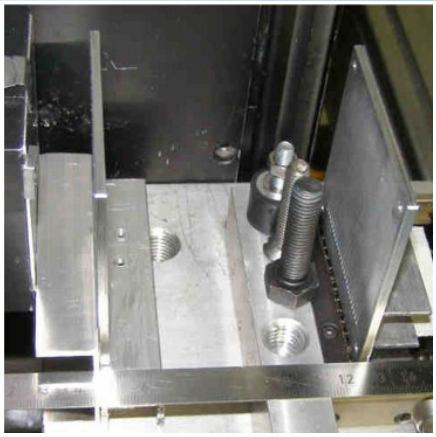

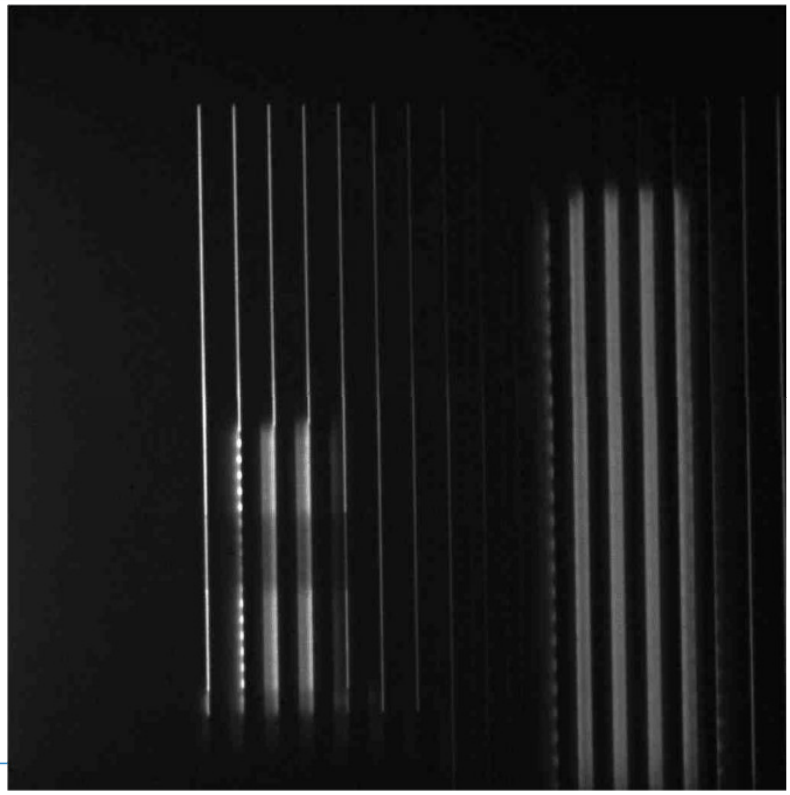

Three screws in 60 mm distance from the detector-sided grid.

The stainless-steel screw in the center delivers no signal.

The stainless-steel nut decreases the signal of the steel screw (left).





Three screws in 20, 45 and 60 mm distance from the detector-sided grid.

The increasing signal proves that it consists of small-angle scattering.

Perfect adjustment of the grids exists only in the beam center

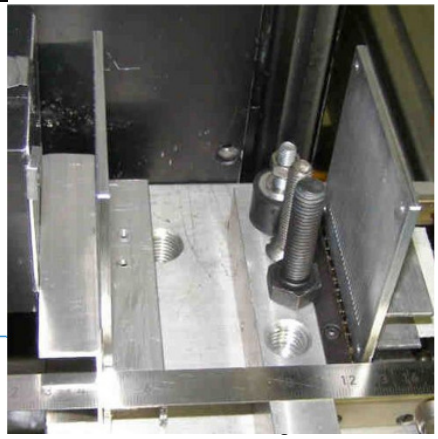

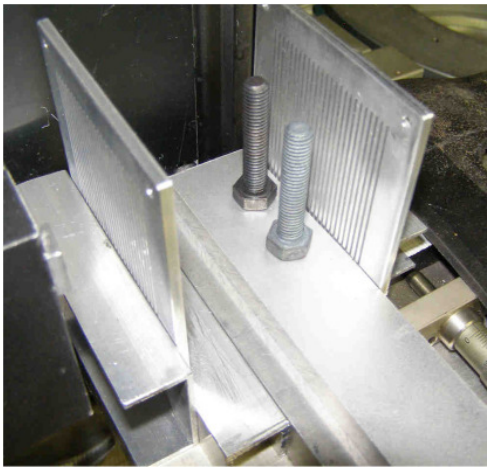

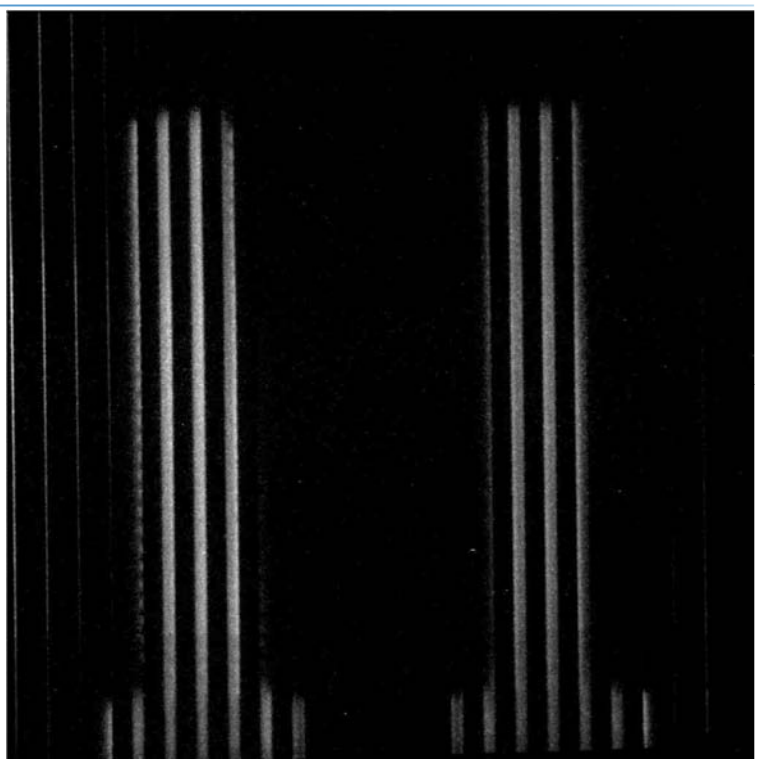

Two steels screws.

The right one has been heat treated, healing small grains – and delivering a weaker scatter signal.





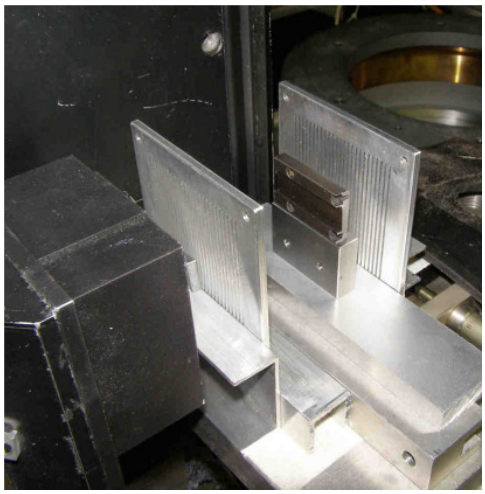

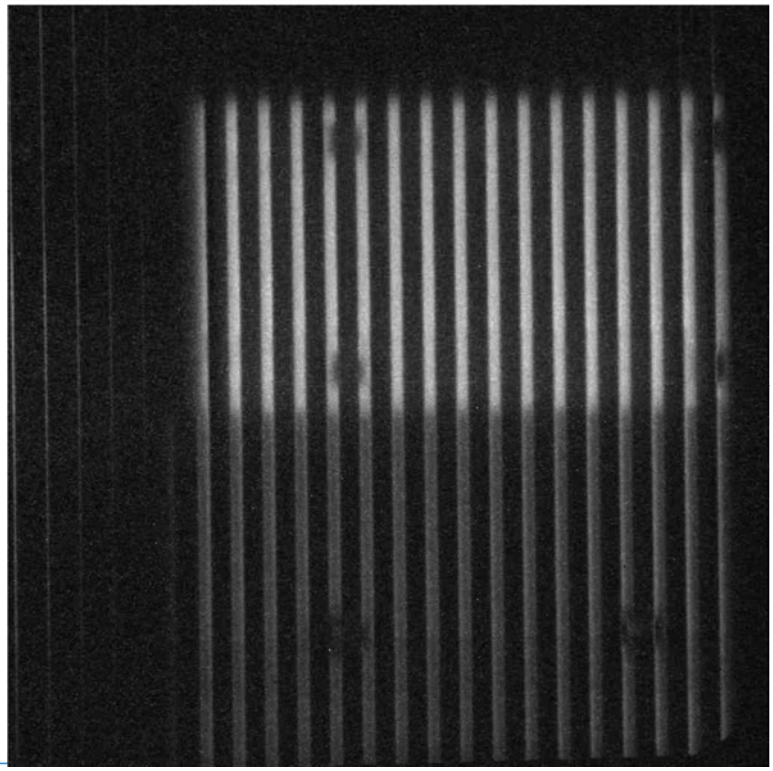

Two plates of steel (top) and stainless steel.
The stainless steel has no precipitations and delivers a weak signal.

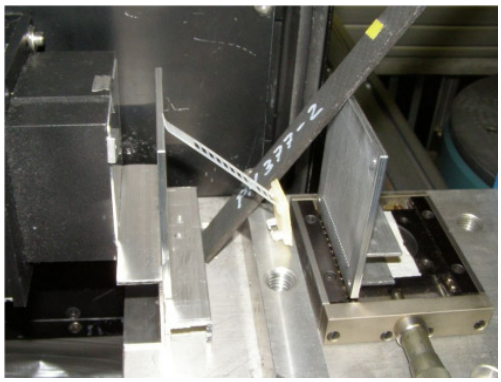

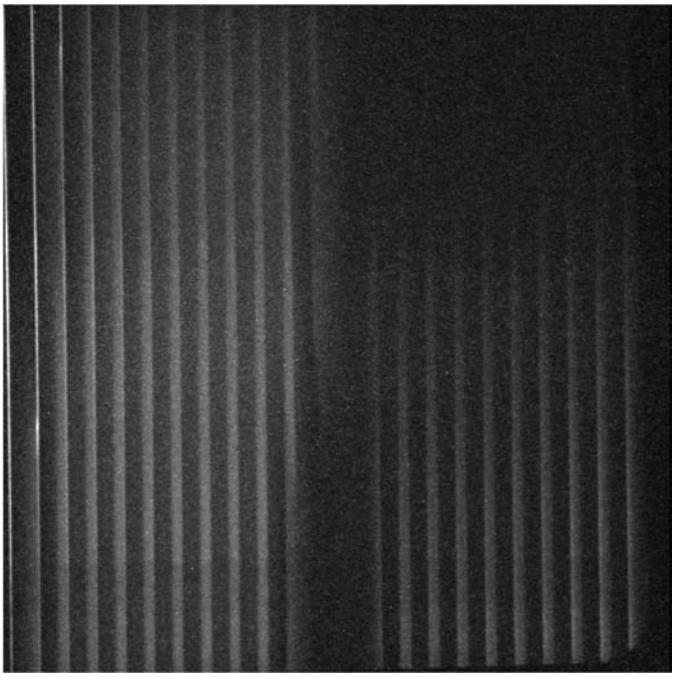

A strip of carbon fiber matrix and a plastic strip deliver a strong scatter signal.

Part of the carbon matrix consists of resin containing hydrogen and delivers bigger scatter angles - intensity decreases with distance.





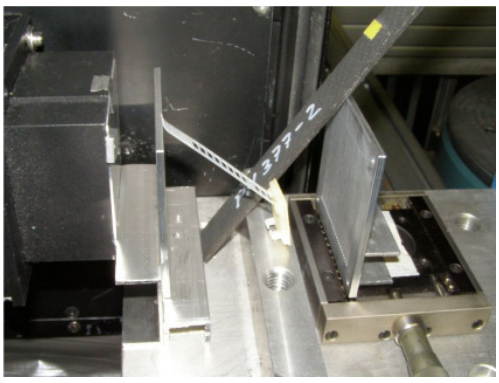

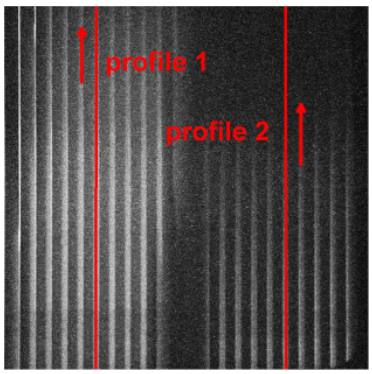


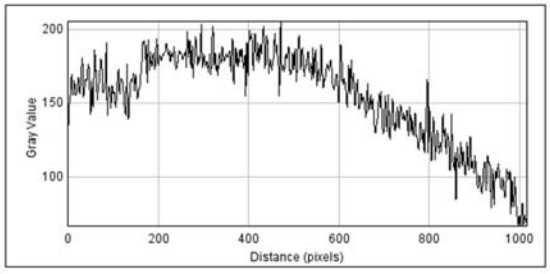


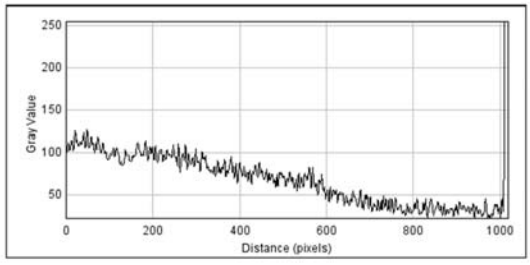


A strip of carbon fiber matrix and a plastic strip deliver a strong scatter signal.

Part of the carbon matrix consists of resin containing hydrogen and delivers bigger scatter angles - intensity decreases with distance.

## Quantitative view:

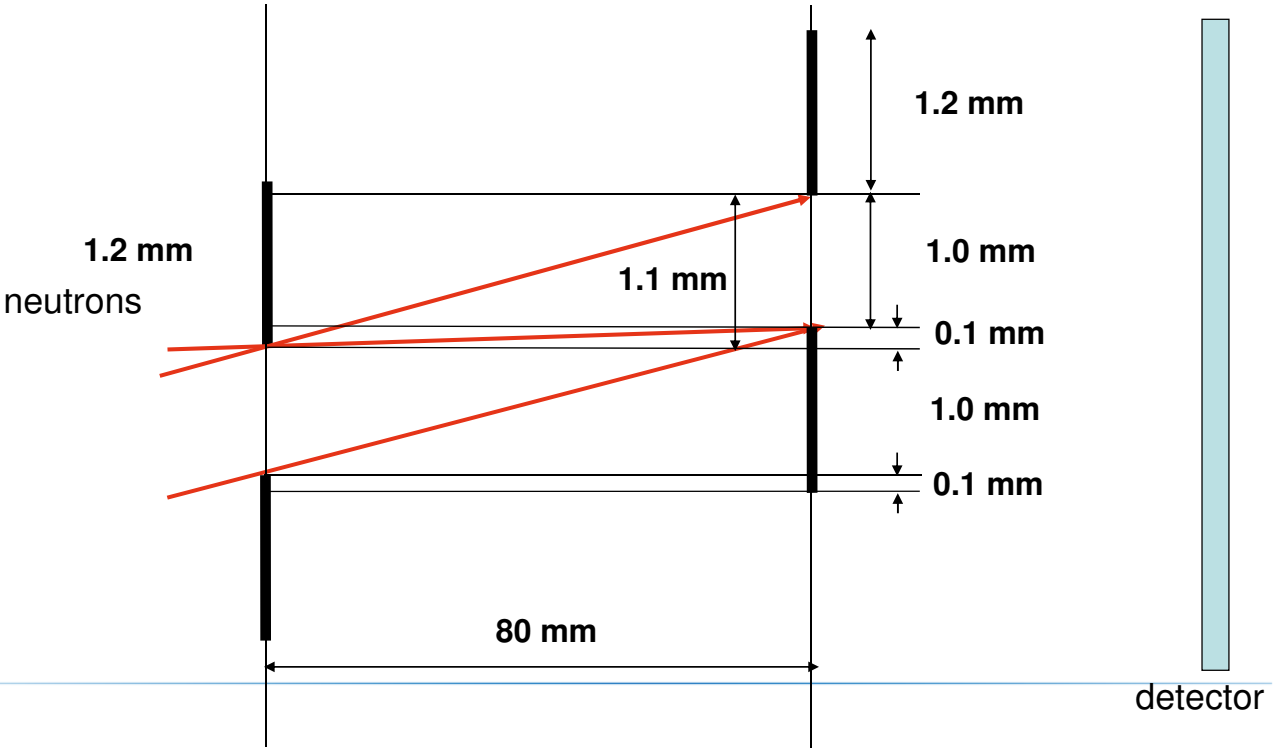






# Quantitative view:

**For transmission of incoming beam:**

**First slit:**
**min. angle: arctan 0.1mm/80mm = 0.07°**
**max. angle: arctan 2.1mm/80mm = 1.50°**

**Second slit:**
**min. angle: arctan 2.3mm/80mm = 1.65°**
**max. angle: arctan 3.8mm/80mm = 2.36°**

**The incoming beam has L/D=800**
**with L=1600 cm and D=2 cm,**
**which gives 0.07° divergency on the beam axis.**

**But: The beam spreads to >20cm.**

- **3 cm off the beam axis, the deviation is 0.1° +/-0.07°**
- **Even with accurate adjustment, there will be edges visible in the image**

# Quantitative view with sample:

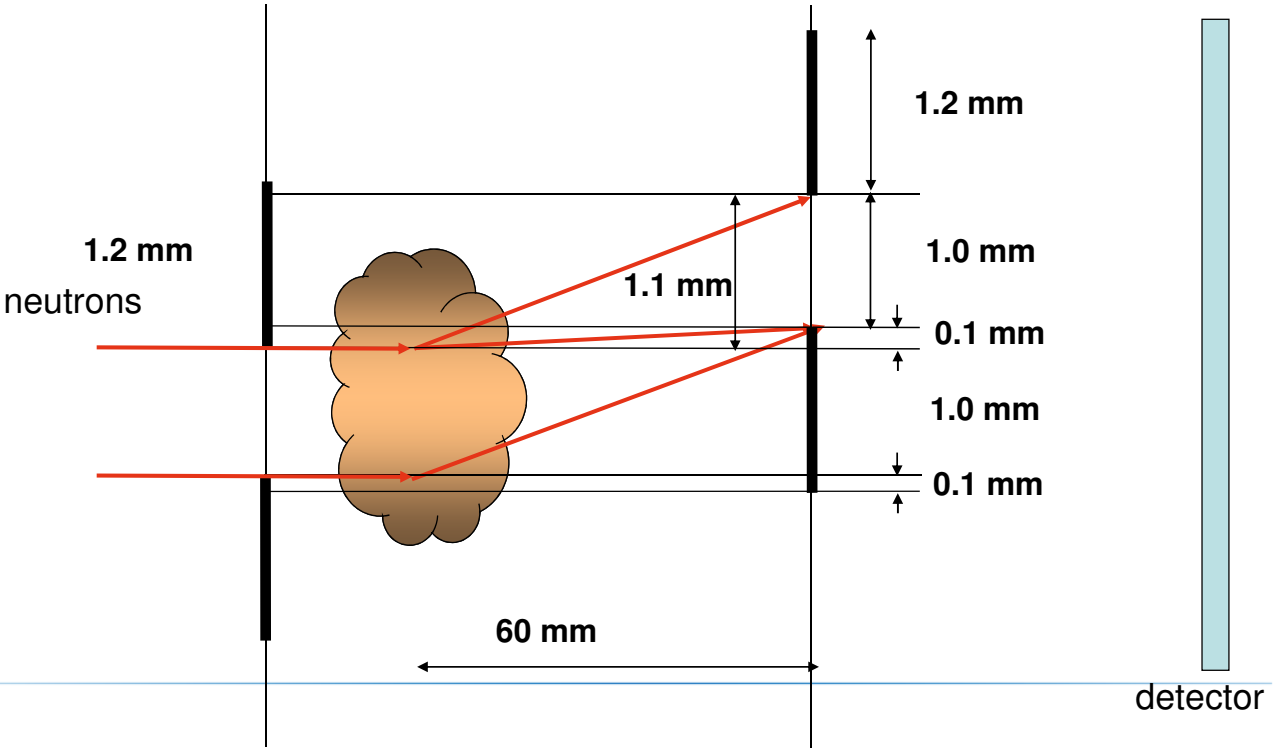






# Quantitative view with sample:

**For transmission of scattered neutrons:**

**60 mm distance sample to grid:**

**First slit:**
**min. angle: arctan 0.1mm/60mm = 0.10°**
**max. angle: arctan 1.1mm/60mm = 1.05°**

**Second slit:**
**min. angle: arctan 2.3mm/60mm = 2.20°**
**max. angle: arctan 4.3mm/60mm = 4.10°**

**45 mm distance sample to grid:**

**First slit:**
**min. angle: arctan 0.1mm/45mm = 0.13°**
**max. angle: arctan 1.1mm/45mm = 1.40°**

**Second slit:**
**min. angle: arctan 2.3mm/45mm = 2.93°**
**max. angle: arctan 4.3mm/45mm = 5.46°**

**20 mm distance sample to grid:**

**First slit:**
**min. angle: arctan 0.1mm/20mm = 0.29°**
**max. angle: arctan 1.1mm/20mm = 3.15°**

**Second slit:**
**min. angle: arctan 2.3mm/20mm = 6.56°**
**max. angle: arctan 4.3mm/20mm = 12.13°**

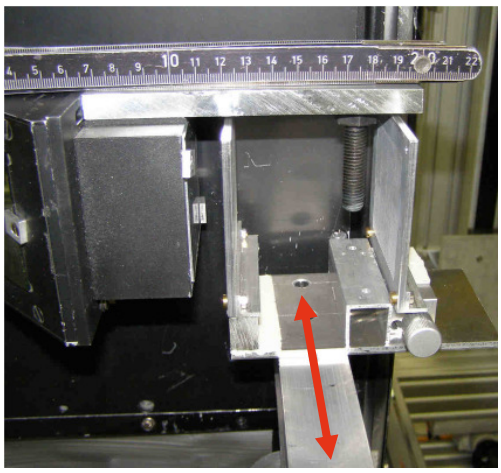

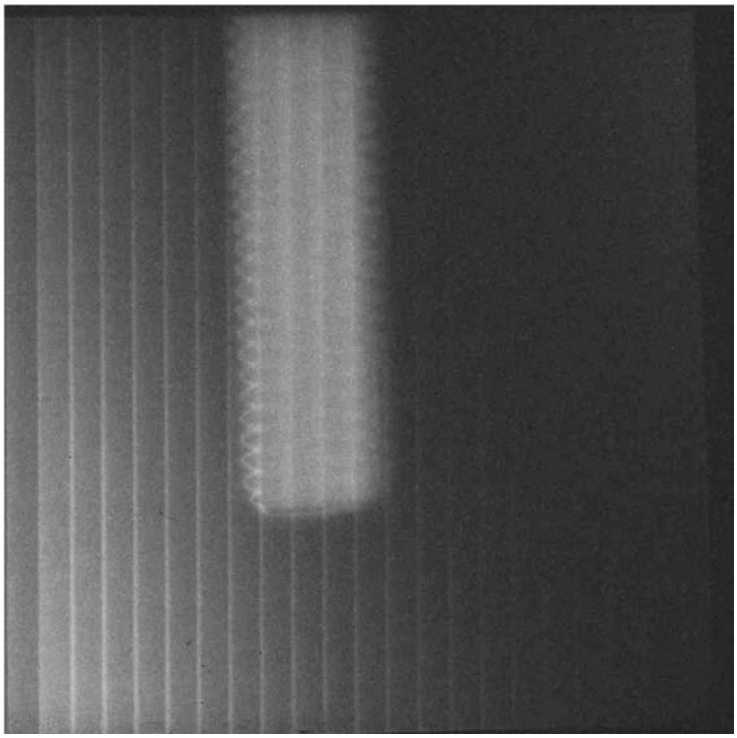

A periodic scanning motion of both grids delivers a full scatter picture.
Even the thread of the M8 screw is visible, proving small-angle scattering.
Second-slit scattering seems to play no major role.





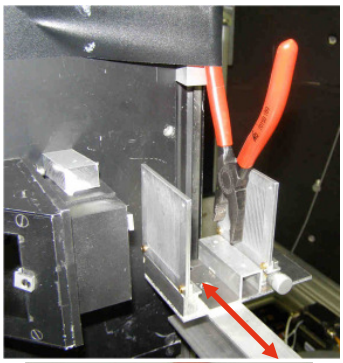

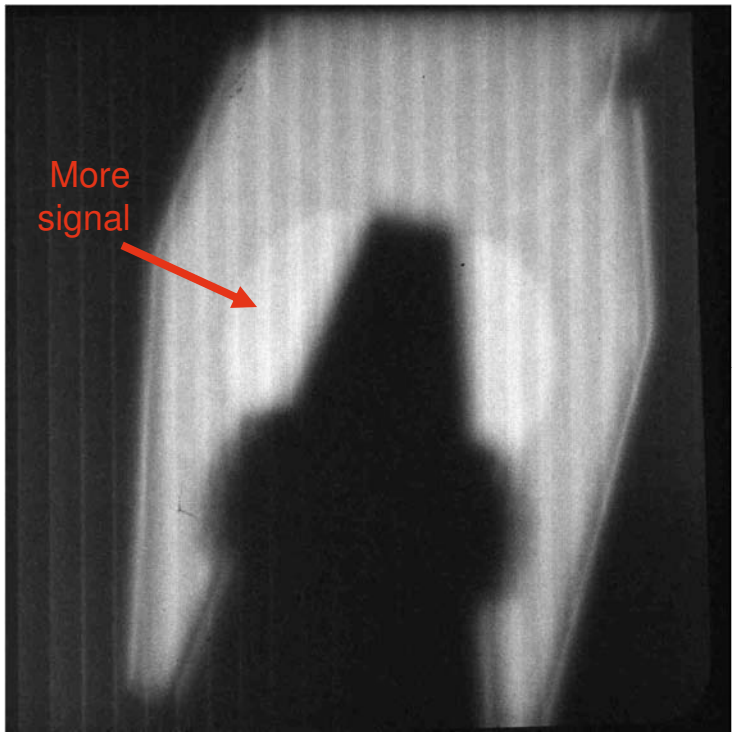


A pair of pliers shows a stronger signal from the thinner parts:
Less self-absorption!

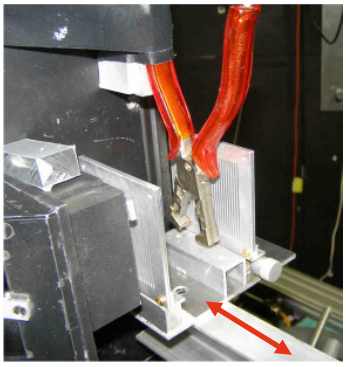

A lot of details are visible in this insulation cutter.





# Conclusion 1

The first experiment at hand delivered surprising image information on a macroscopic scale.

Detailed decription of the geometric setup is still to be combined with small-angle therotical description.

The scanning movement of the grids clearly has a visible impact on the homogeneity and angular range of the transmitted scatter intensity and should be optimised both in amplitude and shape of movement

(currently linear movement with turning points,

sinusoidal movement envisaged)

# Conclusion 2

The gap between neutron imaging and classical scattering techniques is getting smaller.

Neutron imaging can help to determine the homogeneity of samples for scattering experiments,

Scattering effects deliver new information in neutron imaging.

**Any ideas to further combine the benefits from the complementary information are welcome!**





After this first impression,
it is now up to you to find
applications for neutron imaging
in your research fields.

We will gladly help, and try new things.